Russian Chemical Reviews **77** (5) 467 – 486 (2008) © 2008 Russian Academy of Sciences and Turpion Ltd

DOI 10.1070/RC2008v077n05ABEH003766

Non-stoichiometric s-, p- and d-metal diborides: synthesis, properties and simulation

A L Ivanovskii, I R Shein, N I Medvedeva

Contents

I.	Introduction	467
II.	Synthesis and properties of non-stoichiometric s-, p- and d-metal diborides	468
III.	Simulation of non-stoichiometric phases $M_{1-x}B_2$	472
IV.	Conclusion	483

Abstract. The results of recent studies on the synthesis, properties and simulation of the electronic structures of metal diborides are described systematically. The discovery in 2001 of superconductivity in MgB_2 with the critical transition temperature $T_c \approx 39$ K can be considered as the starting point of intensive research on diborides. The discovery of cationic sublattice non-stoichiometry for a series of s-, p- and d-metal diborides with the AlB_2-type structure was among the most interesting results. For some non-stoichiometric diborides, the homogeneity regions can be rather broad. Metal vacancies present in the diborides cause significant changes in their physicochemical properties. Methods of synthesis of cation-deficient s-, p- and d-metal diborides are discussed and the results of experimental and theoretical studies of the effect of cationic vacancies on the properties of these compounds are analysed. The bibliography includes 221 references.

I. Introduction

A perfectly ordered crystalline state of solid-phase systems at $T > 0$ K is unattainable. Non-stoichiometry, as a consequence of violation of a regular crystal structure due to the presence of point defects, is characteristic of all compounds in the condensed state. A general indication of non-stoichiometry is inconsistence between the chemical composition and the number of sites in the crystal sublattices that can be observed experimentally. In other words, classification of all compounds into stoichiometric and non-stoichiometric ones is based on the possibility of experimental observation of phenomena that are due to the presence of lattice defects.

A L Ivanovskii, I R Shein, N I Medvedeva Institute of Solid State Chemistry, Urals Branch of the Russian Academy of Sciences, ul. Pervomaiskaya 91, 620041 Ekaterinburg, Russian Federation. Fax (7-343) 374 44 95, tel. (7-343) 374 53 31, e-mail: ivanovskii@ihim.uran.ru (A L Ivanovskii), tel. (7-343) 362 31 15, e-mail: shein@ihim.uran.ru (I R Shein), tel. (7-343) 362 35 54, e-mail: medvedeva@ihim.uran.ru (N I Medvedeva)

Received 16 January 2008
Uspekhi Khimii **77** (5) 491 – 511 (2008); translated by A M Raevskiy

Lattice vacancies are one of the most abundant types of point defects in crystals. The presence of lattice vacancies causes significant changes in the properties of non-stoichiometric compounds in their homogeneity regions. For instance, non-stoichiometric phases with very broad homogeneity regions (to 30 at.% – 55 at.%) with respect to the non-metal sublattice are available;[1] these are cubic (*B*1 type) Group III – V d-metal carbides, nitrides and oxides.[1] The properties of these compounds can change fundamentally depending on the number of carbon, nitrogen or oxygen vacancies. Controlled introduction of specified concentrations of lattice vacancies (and related effects of atomic vacancy ordering) are considered as a method of design of materials with preset characteristics.[1,2]

In contrast to the systems mentioned above, many metal borides have very narrow homogeneity regions under equilibrium conditions.[3–13] Studies on the properties of metal borides have long been carried out ignoring the non-stoichiometry effects due to the presence of structural vacancies .

The discovery in 2001 of superconductivity in magnesium diboride[14] with the critical transition temperature $T_c \approx 39$ K can be considered as the starting point of modern intensive research of metal diborides (MB_2) and related materials.[15–24] In particular, it was found that, along with the presence of impurities (carbon or other elements) or linear defects and microstress in crystals, non-stoichiometry in the magnesium sublattice also negatively influences the T_c values of MgB_2 samples.[22]

To date, cationic non-stoichiometry in a number of s-, p- and d-metal diborides can be considered proved. For instance, vacancies in the Mg sublattice can be present in $Mg_{1-x}B_2$ ($x \approx 0.04 – 0.05$) samples;[25,26] they can also appear in the Mg sublattice upon doping the boron sublattice with carbon [compositions $Mg_{1-x}(B_{1-y}C_y)_2$, where $x \leqslant 0.1$][27] or in the presence of oxygen.[28] Much higher concentrations of vacancies in the metal sublattice were observed for aluminium diboride ($Al_{1-x}B_2$, $x \approx 0.1 – 0.11$)[29,30] and especially for niobium and tantalum diborides ($Nb_{1-x}B_2$ and $Ta_{1-x}B_2$, $x = 0.01 – 0.5$).[31]

The presence of lattice vacancies is responsible for significant changes in the structural, electrophysical and some other physicochemical properties of metal borides. The influence of vacancies on particular properties of various borides can be opposite in character. For instance, the superconductivity in

MgB_2 is due to strong electron–phonon coupling involving anharmonic phonon modes E_g and quasi-planar near-Fermi σ-electron bands of planar boron sheets (see reviews [19–21]); therefore, any violation of the crystal structure (including those caused by the presence of vacancies) will negatively influence the T_c value. Indeed, the critical temperature T_c of magnesium diboride decreases by about 2–3 K in the presence of 5% Mg vacancies.[22] Contrary to this, 'perfect stoichiometric' niobium diboride $NbB_{2.0}$ shows no superconductivity (up to $T < 2.5$ K),[32–34] whereas cation-deficient samples $Nb_{1-x}B_2$ have $T_c \sim 9$ K.[31, 35–38]

In addition to diborides, cationic non-stoichiometry was found for other boride phases [*e.g.*, hexaborides $M_{1-x}B_6$ (Ref. 39) or pentaborides $M_{2-x}B_5$ (Refs 40–48)]. Yet another type of lattice defects in crystalline borides, namely, vacancies in the boron sublattice, is less characteristic of metal diborides. This can easily be explained taking account of specific features of chemical bonds in the MB_2 phases (covalent bonds in hexagonal boron sheets are the strongest).[12–19, 49–59]

In this review, we summarised the available information on the synthesis of cation-deficient s-, p- and d-metal diborides reported since 2001 and analysed the results of experimental and theoretical studies of the effect of cationic vacancies on the properties of AlB_2-type diborides.

II. Synthesis and properties of non-stoichiometric s-, p- and d-metal diborides

To date, the most reliable experimental data on cationic non-stoichiometry were obtained for MgB_2, AlB_2, NbB_2, TaB_2 and MoB_2. Methods of synthesis and the properties of stoichiometric diborides are well documented (see handbooks and reviews [3–11, 60–62]).

Recall that stoichiometric AlB_2-type metal diborides have a hexagonal structure (space group $D^1_{6h}-P6/mm$) and one formula unit in the unit cell ($Z = 1$).[3–11] Boron atoms occupy the centres of trigonal prisms formed by metal atoms (M). Prisms' faces contact one another and form a three-dimensional packing. The coordination number and coordination polyhedron for the M atoms are 20 and $[MB_{12}M_8]$, respectively. The respective parameters for boron atoms are 9 and $[BM_6B_3]$. The atomic positions in the unit cell are as follows: 1M(*a*): 0, 0, 0; 2B(*d*): 1/3, 2/3, 1/2 and 2/3, 1/3, 1/2. The interatomic distances are $B-B = a/\sqrt{3}$; $B-M = (\sqrt{a^2/3} + \sqrt{c^2/4})$, $M-M = a$ (in-plane), where a and c are the lattice constants. Structurally, the MB_2 systems comprise of planar hexagonal metal nets and graphite-like boron sheets alternating in the order .../M/B_2/M/B_2/... (Fig. 1).

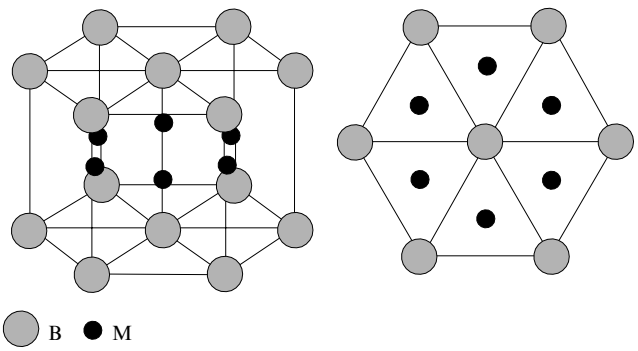


Figure 1. Crystal structure of AlB_2-type metal diborides.

1. The Mg–B system. Magnesium diboride MgB_2

Studies of phase equilibria (Fig. 2) in the Mg–B system revealed three main phases, namely, MgB_2, MgB_4 and MgB_7. Higher magnesium borides MgB_{12} (Ref. 63) and MgB_{20} (Ref. 64) were also reported.

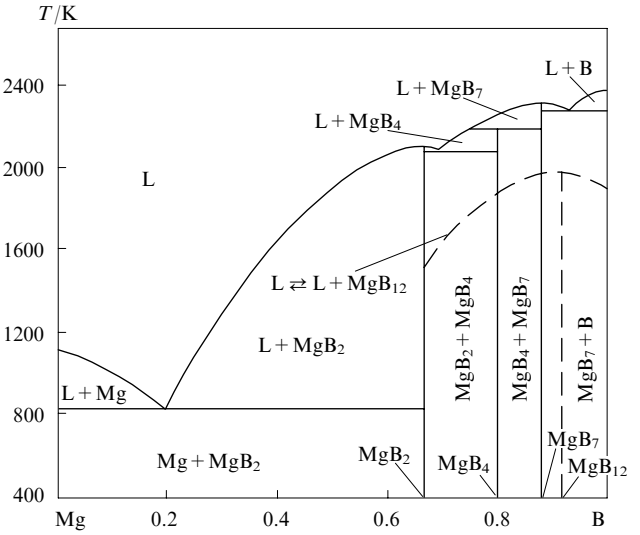


Figure 2. Phase diagram of the Mg–B system.[63]

Polycrystalline samples of superconducting MgB_2 are most often prepared by solid-phase synthesis from elemental B and Mg.[16, 18, 20, 22] The available procedures differ in compositions of raw materials, atmosphere and regimes of pressure and heat treatment. The methods of preparation of polycrystalline MgB_2 include mechanochemical synthesis, crystallisation from solutions, self-propagating synthesis and treatment of crystalline or amorphous boron with magnesium vapour.[16, 18, 20, 22, 63–73] Methods of growth of single-crystalline MgB_2 (Refs 74–78) and magnesium diboride films were also proposed. In the latter case, one can use an *ex situ* or an *in situ* procedure. The *ex situ* processes involve coating of substrate with boron films in the first stage and subsequent saturation of the films with magnesium. In the *in situ* processes, MgB_2 films are prepared during one experiment.[79–93] Nanocrystalline MgB_2 samples were also synthesised.[94–96]

The properties of MgB_2 (including the superconductivity parameters) are affected by not only dislocations, packing defects,[97] mesoscopic inhomogeneity regions,[98] inter- and intra-grain boundaries,[99] various radiation-induced defects [100] or substitutional impurities,[101] *etc.*, but also structural defects, namely, vacancies in the magnesium sublattice.[25, 26, 102–107] In particular, a percolation theory of superconductivity in $Mg_{1-x}B_2$ was proposed, which assumes coexistence of stoichiometric $Mg_{1.0}B_2$ and a diboride phase formed upon clustering of magnesium vacancies and enriched with cationic defects.[103, 104]

Cationic vacancies in the MgB_2 lattice can appear:

— during the synthesis of magnesium diboride samples [25, 26, 102–107] depending on the kinetic and thermodynamic conditions;

— on doping $Mg_{1-x}B_2$ with impurities (*e.g.*, carbon or oxygen);[27, 28]

— in the case of targeted creation of vacancies in the MgB_2 samples by, *e.g.*, irradiation.[97, 108–117]

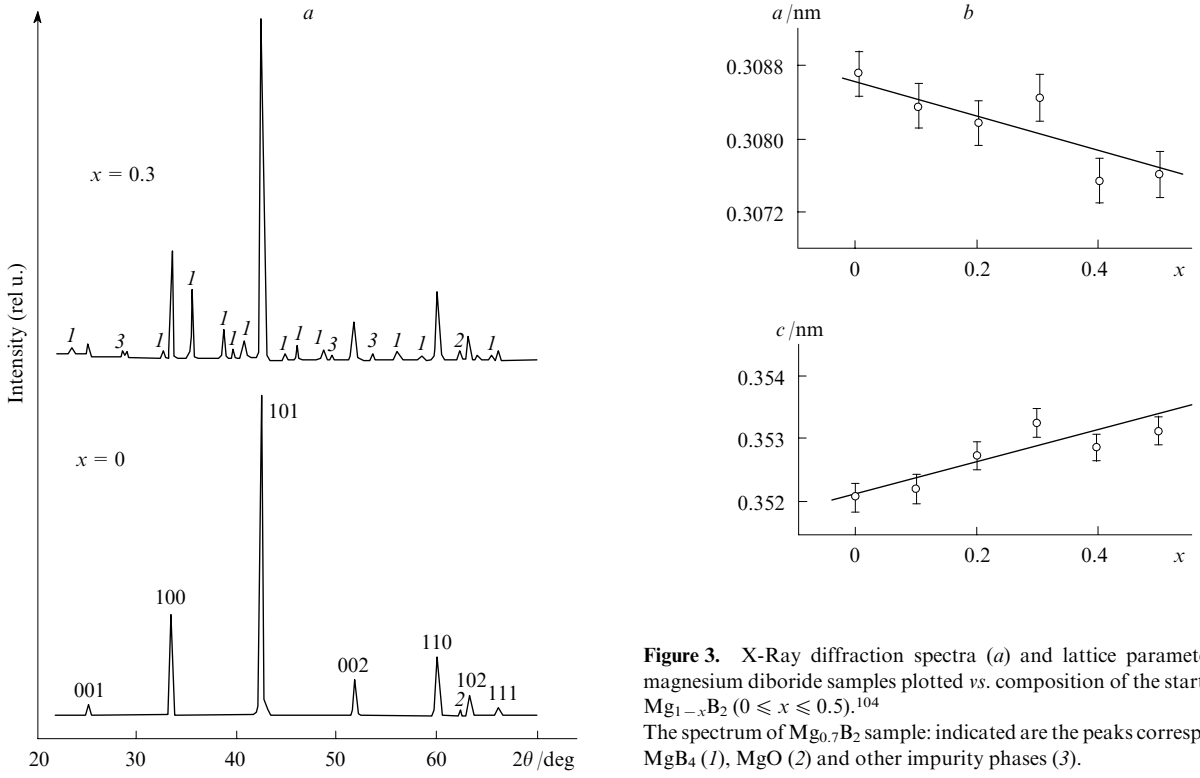


Figure 3. X-Ray diffraction spectra (*a*) and lattice parameters (*b*) of magnesium diboride samples plotted *vs*. composition of the starting batch $Mg_{1-x}B_2$ ($0 \leqslant x \leqslant 0.5$).[104]
The spectrum of $Mg_{0.7}B_2$ sample: indicated are the peaks corresponding to MgB_4 (*1*), MgO (*2*) and other impurity phases (*3*).

Studies [105, 118] of the dependence of the structure and properties of magnesium diboride samples prepared by solid-phase synthesis on the composition of starting raw material $Mg_{1-x}B_2$ ($0 \leqslant x \leqslant 0.5$) revealed the formation of two-phase samples ($MgB_2 + MgB_4$) containing small amounts of MgO and other impurity phases (Fig. 3) under magnesium deficiency conditions.

According to X-ray diffraction data, an increase in x (B : Mg ratio) in the composition of the raw material causes different-type changes the MgB_2 lattice constants, namely, the interplanar distance between boron sheets (parameter c) increases, whereas the parameter a decreases (see Fig. 3). These changes were attributed [101] to the presence of vacancies in the magnesium sublattice (and, probably, to a small amount of interstitial boron atoms). It is noteworthy that the lattice constants of the second phase (MgB_4) remain unchanged within the limits of measuring error.[105, 118]

Studies [25, 26, 101–107, 119–121] of single-phase $Mg_{1-x}B_2$ samples showed that the homogeneity region of hexagonal magnesium diboride is rather narrow ($0 \leqslant x \leqslant 0.1$) and that the samples with the composition $Mg_{0.9}B_2$ (Ref. 102) are multiphase and have inhomogeneous microstructure, irregular grain sizes and high porosity (Fig. 4). In the homogeneity region of the $Mg_{1-x}B_2$ system, the critical temperature decreases by 1–3 degrees with an increase in the concentration of cationic vacancies.[22, 119–121]

Radiation-induced defect formation in MgB_2 under irradiation with protons, neutrons, γ-quanta, electrons and heavy ions was studied experimentally.[108–117] In most cases, rather heavy irradiation doses were applied (from 5×10^{17} to 5×10^{19} cm^{-2}), at which radiation-induced point defects recombine with the formation of extended defects.

A systematic study of the formation of point defects (vacancies) in MgB_2 samples under electron irradiation (average irradiation energy $E \sim 10$ MeV) was carried out.[117] The lattice constants, intensities and width of X-ray diffraction lines were determined at different irradiation doses (from 0 to

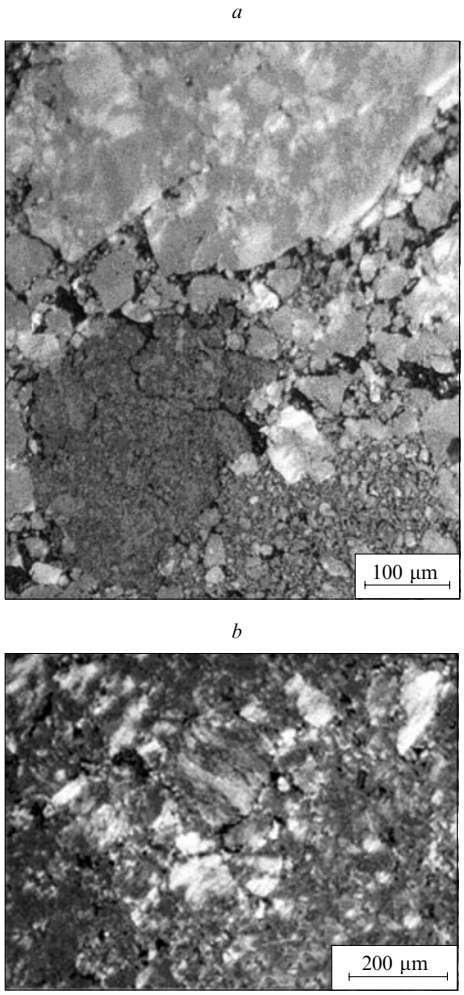


Figure 4. Morphology of $Mg_{0.9}B_2$ (*a*) and $Mg_{1.1}B_2$ (*b*) samples.[105]

5×10^{16} cm^{-2}). Based on analysis of changes in these parameters, it was concluded [114] that in the initial stage of irradiation of MgB_2 with high-energy electrons most vacancies appear in the magnesium sublattice and then in the boron sublattice; at an irradiation dose of $\geqslant 5 \times 10^{16}$ cm^{-2}, vacancies appear in both sublattices. Antisite defects (Mg $\leftrightarrow$ B positional exchange) are unlikely (mainly, due to considerable difference between the ionic radii of magnesium and boron).

The results of experimental studies showed that hexagonal MgB_2 can contain a rather low concentration of cationic vacancies (up to 5%–9%) and that the presence of vacancies in the sample causes insignificant changes in the lattice constants and deteriorates the superconductivity characteristics of MgB_2. The assumptions of possible clustering of Mg vacancies (*e.g.*, at grain boundaries with the formation of a specific 'defective phase' [106, 107]) and of the presence of other types of point defects (vacancies in the boron sublattice or interstitial boron and magnesium atoms) in MgB_2 have not been experimentally substantiated so far and seem to be debatable.

2. The Al–B system. Aluminium diboride AlB_2

Hexagonal AlB_2 seems to be the first diboride phase for which cationic non-stoichiometry was assumed [122] based on the deviation of the measured density of the sample from the theoretical value and the composition $Al_{0.9}B_2$ proposed.

The structure and certain properties of $Al_{1-x}B_2$ were studied in detail [29] using single-crystalline samples synthesised by two different methods from Al–B melts. In both cases, hexagonal crystals (space group $P6/mmm$) with the same lattice constants $a = 0.30050(1)$ nm and $c = 0.32537(8)$ nm and the density $\rho_{exp} = 2.9(1)$ g cm^{-3} were obtained. The experimental density is in agreement with the theoretical value $\rho_{theor} = 2.98(2)$ g cm^{-3} calculated for the composition $Al_{0.894}B_2$ and with other published data on the density of aluminium diboride samples (2.84 and 2.955 g cm^{-3}, Ref. 29).

Since the aluminium diboride samples were synthesised [29] from Al-enriched melts, it was postulated that the composition $Al_{0.894}B_2$ ($\sim Al_{0.9}B_2$) corresponds to the maximum possible content of aluminium in the single-phase diboride. The compositions of polycrystalline aluminium diboride samples established from the X-ray emission spectroscopy and X-ray absorption spectroscopy data ($Al_{0.93}B_2$, Ref. 115) and from diffraction data obtained in synchrotron experiments ($Al_{0.89}B_2$, Refs 30 and 123) are in good agreement with this conclusion. Additional arguments in favour of the presence of Al vacancies and non-equivalent environment of boron atoms in $Al_{1-x}B_2$ were provided by ^{11}B NMR spectroscopy [29] and by the results of comparison of the theoretical and experimentally measured phonon modes E_{2g}.[30]

3. The Nb–B system. Niobium diboride NbB_2

In contrast to the s- and p-metal diborides $M_{1-x}B_2$ ($0 \leqslant x \leqslant 0.1$, see above) with narrow homogeneity regions, the corresponding phases of d-metal diborides can contain much higher concentrations of cationic vacancies.[31, 35–38, 124–127] Among the d-metal diborides, the diborides $Nb_{1-x}B_2$ are best studied.[35–38, 125–133]

$Nb_{1-x}B_2$ are usually synthesised from elemental B and Nb. For instance, polycrystalline NbB_{2+y} ($y = 0$, 0.03, 0.1) samples were prepared [126] from the corresponding mixtures of niobium powders and crystalline boron pressed into pellets that were placed in quartz tubes and annealed at 1000 °C and at pressures $P < 3.0 \times 10^5$ Torr for 30 h. Mixtures of niobium and amorphous boron were also placed [31, 125] in a boron nitride tube that was heated to 800–1200°C and then kept at this temperature for 0.5–2 h at a pressure $P \approx 1$–6 GPa.

Another method of synthesis of boron-enriched samples NbB_{2+y} (B : Nb = 2.0–2.6) assumes [36] the use of commercially available niobium diboride (precursor) mixed with elemental boron. The corresponding pellets were placed in a steel tube and kept at 1000 °C in an inert atmosphere (Ar) for 3 h.

Structural studies showed [31, 36, 38, 134–136] that, as in the case of magnesium diboride, the lattice constants of NbB_2 change oppositely with an increase in the B : Nb ratio. Namely, the parameter a decreases, whereas the parameter c increases (Fig. 5) and the unit cell volume decreases. Boron-rich phases $Nb_{1-x}B_2$ were analysed [38] using three structural models including (*1*) defect-free boron sublattice and the presence of vacancies in the Nb sublattice; (*2*) insertion of extra boron atoms into interstices and (*3*) occupation of vacant sites in the niobium sublattice by the extra boron atoms. Comparison [38] of the results of calculations of diffraction spectra carried out using these models with experimental data revealed preferableness of model *1*, *i.e.*, the presence of cationic vacancies in $Nb_{1-x}B_2$. Ordering of vacancies was also simulated;[38] however, a comparison with experimental diffraction lines revealed no superstructure, which indicates a disordered vacancy distribution in the Nb sublattice.

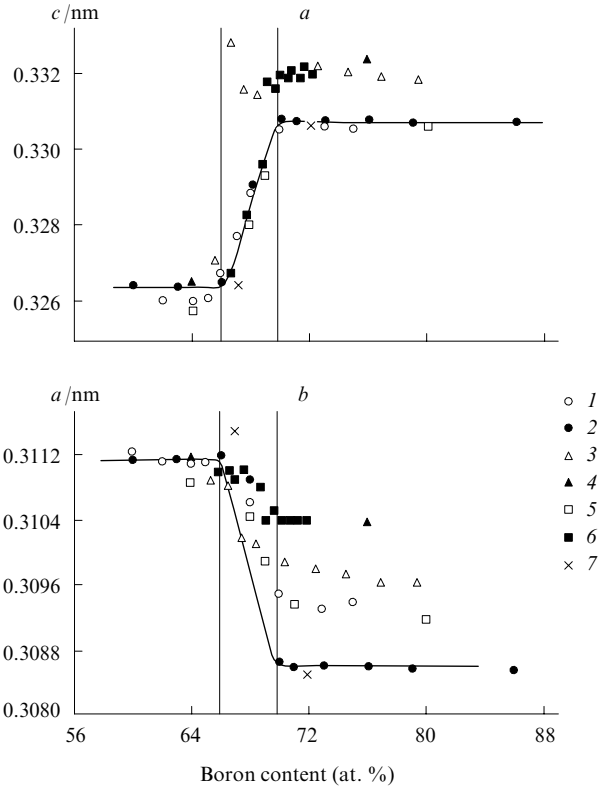


Figure 5. Lattice parameters c (*a*) and a (*b*) plotted *vs.* boron content for niobium diboride .
Data were taken from Refs 134 (*1*), 38 (*2*), 31 (*3*), 135 (*4*), 136 (*5*), 36 (*6*) and 147 (*7*).

Not only the structural parameters, but also the superconductivity parameters and magnetic properties of $Nb_{1-x}B_2$ depend on the B : Nb ratio (Fig. 6).[31, 36, 38, 134–137]

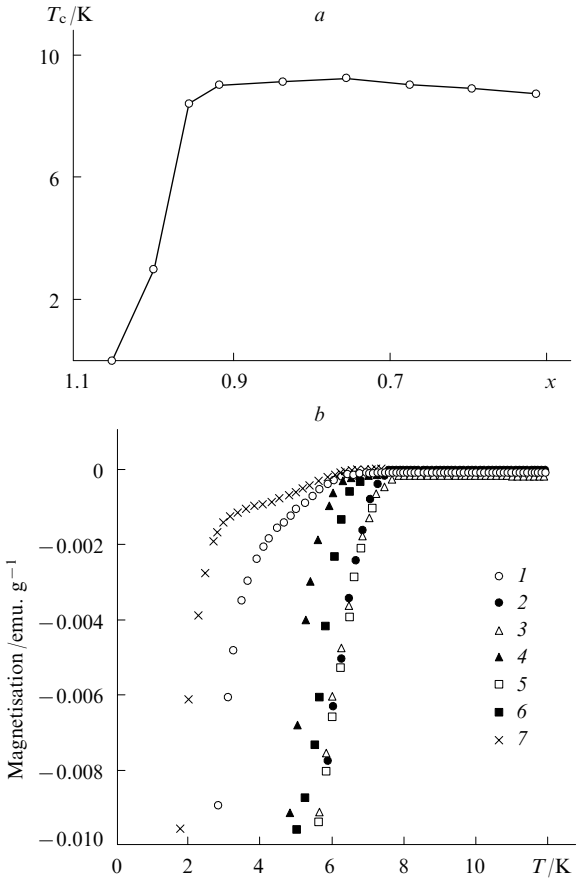


Figure 6. Critical temperature T_c (*a*)[31] and magnetisation (*b*)[128] of $Nb_{1-x}B_2$ plotted *vs.* *x*.
x = 0.67 (*1*), 0.80 (*2*), 0.91 (*3*), 0.95 (*4*), 1.00 (*5*), 1.05 (*6*), 1.11 (*7*).

4. The Ta – B system. Tantalum diboride TaB_2

The syntheses of both stoichiometric and non-stoichiometric tantalum diboride were reported.[31, 138–141] Polycrystalline samples of cation-deficient $Ta_{1-x}B_2$ ($0 \leqslant x \leqslant 0.24$) were prepared[31] under high pressure and temperature (P = 5 GPa, T = 1200 °C) from mixtures of tantalum and amorphous boron powders placed in a boron nitride tube. The lattice constants a and c changed almost linearly[31, 141] with the change in the B : Ta ratio (Fig. 7). The lattice constants of $Ta_{1-x}B_2$ ($x > 0.24$) remained unchanged upon an increase in the degree of tantalum deficiency, which indicated attainment of the boundary of the homogeneity region for this phase.

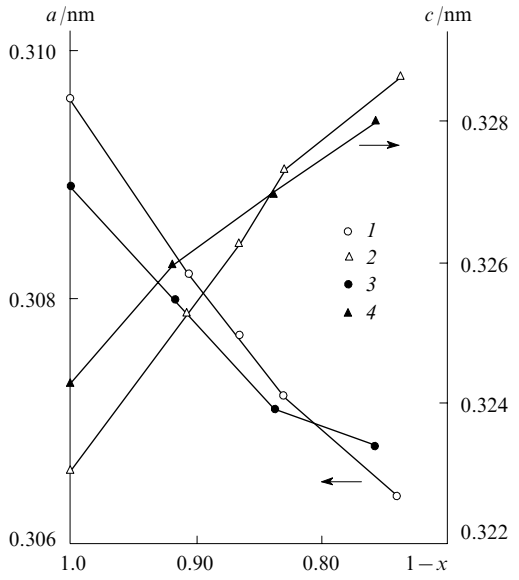


Figure 7. Lattice parameters *a* (*1*, *3*) and *c* (*2*, *4*) plotted *vs.* boron content for tantalum diboride.
Data from Refs 31 (*3*, *4*) and 142 (*1*, *2*).

Magnetic susceptibility measurements showed that T_c ($Ta_{1-x}B_2$) is at most 2 K.[21]

5. The Mo – B system. Molybdenum diboride (MoB_2) and molybdenum pentaboride (Mo_2B_5)

Among the AlB_2-type d-metal diborides, compounds of Group IV metals (Ti, Zr and Hf) are the most stable, whereas the stability of these hexagonal phases formed by Group V and (especially) Group VI d-metals abruptly decreases.[3–11] This can be explained by the changes in the (i) filling of energy bands;[50, 51, 142] (ii) densities of states at the Fermi level[140] and (iii) interatomic bonds[49] or cohesive energies of the systems.[19, 51, 52, 54, 143–145]

Being one of the thermodynamically most unstable AlB_2-type phases, which is near the boundary of the stability region of hexagonal 4d-metal diborides, molybdenum diboride is not unworthy of notice for researchers. The available information on phase equilibria in the Mo – B system[40–48, 146, 147] is contradictory. For instance, two main phases of molybdenum borides have formal compositions Mo : B ≈ 0.4–0.5 (hexagonal MoB_2) and rhombohedral Mo_2B_5 (their structural parameters are listed in Table 1); a number of intermediate molybdenum-

Table 1. Structural parameters and atomic coordinates for two main phases of molybdenum boride (hexagonal MoB_2 and rhombohedral Mo_2B_5).

Phase	Symmetry group	Lattice parameters			Ref.[a]	Atomic positions			
		a/Å	c/Å	c/a		type	x	y	z[b]
MoB_2	*P6/mmm*	3.012	3.330	1.106	148	Mo (1a)	0	0	0
		3.099	3.055	1.005	8	B (2d)	1/3	2/3	1/2
		3.050	3.113	1.010	7				
Mo_2B_5	*R3m*	3.010	20.926	6.953	148	Mo (6c)	0	0	0.076 (0.076)
		3.011	20.930	6.950	7	B(1) (6c)	0	0	0.332 (0.332)
		3.010	20.927	6.953	46	B(2) (6c)	0	0	0.185 (0.182)
						B(3) (3b)	0	0	1/2

[a] Experimental data[7, 8, 46] and results of calculations.[148] [b] Data from Ref. 46 are given in parentheses.

deficient ($Mo_{1-x}B_2$, $Mo_{2-x}B_5$) or boron-deficient (MoB_{2-x}, Mo_2B_{5-x}) phases were also reported. The formation of each phase depends on the method of synthesis and reaction conditions.[40–48, 146–149] For instance, the results of mechanochemical synthesis,[48] *i.e.*, the compositions of various products (MoB_2, Mo_2B_5 or $MoB_2 + Mo_2B_5$), first of all depend on the composition of the starting raw material (B : Mo ratio).

An attempt to synthesise cation-deficient phases $Mo_{1-x}B_2$ under high pressure was reported.[31] This technique was successfully used for preparation of non-stoichiometric diborides $Nb_{1-x}B_2$ and $Ta_{1-x}B_2$ (see above). Samples of compositions $Mo_{1.0}B_2$, $Mo_{0.84}B_2$ were prepared at $P = 5$ GPa and $T = 1100–1200$ °C; however, X-ray diffraction experiments revealed the Mo_2B_5 structural type. Transition to the superconducting state was not detected.

At the same time, non-stoichiometric hexagonal AlB_2-type molybdenum diboride can be stabilised by doping with zirconium [compositions $(Mo_{0.96}Zr_{0.04})_xB_2$, where $1 < x < 0.85$].[147] The possibility of vacancy ordering was suggested,[145] but the intensities of the superstructural peaks in the neutron diffraction experiments were too low for identification of the superstructure. As the concentration of metal vacancies increased, the superconducting transition temperature increased from 5.9 to 8.2 K. Samples of non-stoichiometric $Mo_{1-x}B_2$ stabilised by titanium and hafnium were also synthesised.[145]

6. The Ag – B system. Silver diboride AgB_2

The formation of boron-rich phases (B : M > 1) is not a characteristic feature of noble metal – boron systems.[3–11] Nevertheless, it was reported [150, 151] that, owing to specific energy band structure (increased concentration of near-Fermi σ-like B2p-states [53]), the hypothetic AlB_2-type silver and gold diborides can have electron – phonon coupling constants higher than those of MgB_2 and their critical temperatures T_c can be as high as 50 – 70 K. However, according to another model [152] with inclusion of spin fluctuations, the critical temperature of AgB_2 should be much lower ($T_c < 10$ K).

Information on the synthesis of hexagonal AgB_2 is contradictory. The synthesis of silver diboride (space group $P6/mmm$, lattice constants $a = 3.00$ and $c = 3.24$ Å) was first reported more than four decades ago.[153] More recent attempts [154, 155] to synthesise this phase in the form of polycrystals or thin films by codeposition of Ag and B have failed and it was concluded that AgB_2 is unstable. However, a very recent study [156] revealed the possibility of preparation of high-quality AgB_2 samples by simple solid-phase synthesis involving sintering of pellets pressed from a mixture of silver and boron powders taken in a stoichiometric ratio at $T = 750$ °C in high vacuum over a period of 3 h. We believe that more reliable results were obtained by the authors of study [157] who used laser deposition for the synthesis and subsequent annealing of thin-film Ag/B composite (Fig. 8). The 'silver diboride' samples thus obtained exhibited superconducting properties at ~6.7 – 7.4 K. At the same time, the samples had an inhomogeneous structure with inclusions.[157] The impossibility of preparation of single-phase 'AgB_2' films by magnetron sputtering was also reported.[158] However, since the compositions of the 'AgB_2' samples synthesised [157, 158] varied over a wide range, the possibility of formation of $Ag_{1-x}B_2$ phases with non-stoichiometry in the metal sublattice cannot be excluded *a priori*.

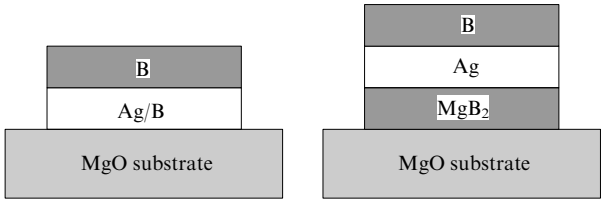


Figure 8. Structure of composite films used as precursors in the synthesis of silver diboride films.[157]

III. Simulation of non-stoichiometric phases $M_{1-x}B_2$

To date, the electronic structure and the nature of interatomic interactions have been studied in detail for many stoichiometric metal diborides including MgB_2 (Refs 16 – 19, 21, 52 – 56, 144, 159 – 169), AlB_2 (Refs 12, 13, 19, 54 – 56, 144, 169 – 173), NbB_2 (Refs 12, 13, 19, 51, 55, 144, 173 – 175), TaB_2 (Refs 13, 19, 51, 173, 175 – 178), MoB_2 (Refs 12, 13, 19, 51, 55, 59, 144, 148, 173, 179) and AgB_2 (Refs 53, 150 – 152, 180).

Their common features are as follows. The valence spectrum of MgB_2 is determined by the B2p states that form four $\sigma(2p_{x,y})$ and two $\pi(2p_z)$ bands. The energy dispersion curves for these states are significantly different (Fig. 9). For the $B2p_{x,y}$ bands, the energy dispersion is maximum along the

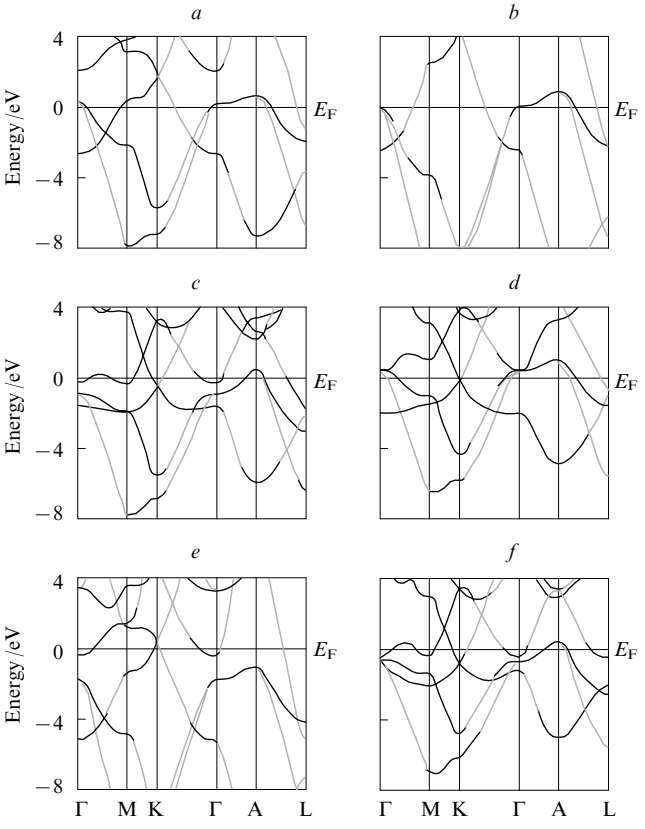


Figure 9. Energy bands of hexagonal diborides MB_2.[55] M = Mg (*a*), Be (*b*), Sc (*c*), Ca (*d*), Al (*e*), Y (*f*).

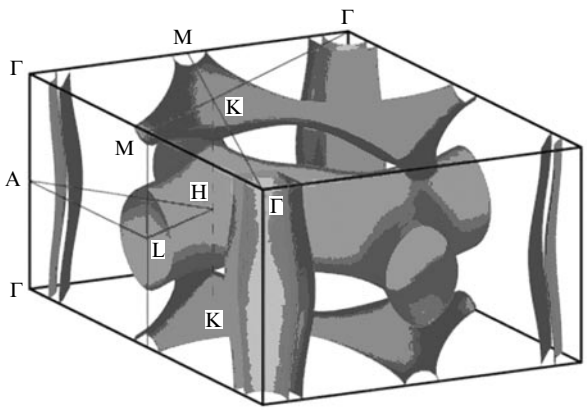


Figure 10. Fermi surface of magnesium diboride.[159]

Γ—K direction. These bands characterise the distribution of boron states within the graphite-like sheets; they are of quasi-two-dimensional (2*D*) character and have flat sections along the Γ—A direction. Two $B2p_{x,y}$ bands intersect the Fermi level (E_F) and contribute largely to the total density of states at the Fermi level [$N(E_F) \approx 30\%$], being responsible for the metal-like properties of the diboride. One of the key features of the electronic spectrum of MgB_2 is energy position of $B2p_{x,y}$ bands; namely, at the Γ point in the Brillouin zone they are higher than E_F and form cylindrical fragments of the hole-type Fermi surface (Fig. 10).

The $B2p_z$ states are oriented normal to the boron sheets; they are responsible for weak interlayer π-bonds. Both π bands intersect the Fermi level and have a maximum dispersion along the Γ—A direction. The magnesium s and p states, as well as the boron s states are admixed to the system of the B2p bands near the edge of the valence band and in the conduction band.

Hexagonal borides of other s-, p- and d-metals have similar electronic spectra.[19] Studies on the electronic structure of the MB_2 phases were focused on the near-Fermi states and on their influence on the superconducting characteristics of these systems. For instance, the fact that BeB_2 exhibits no super-

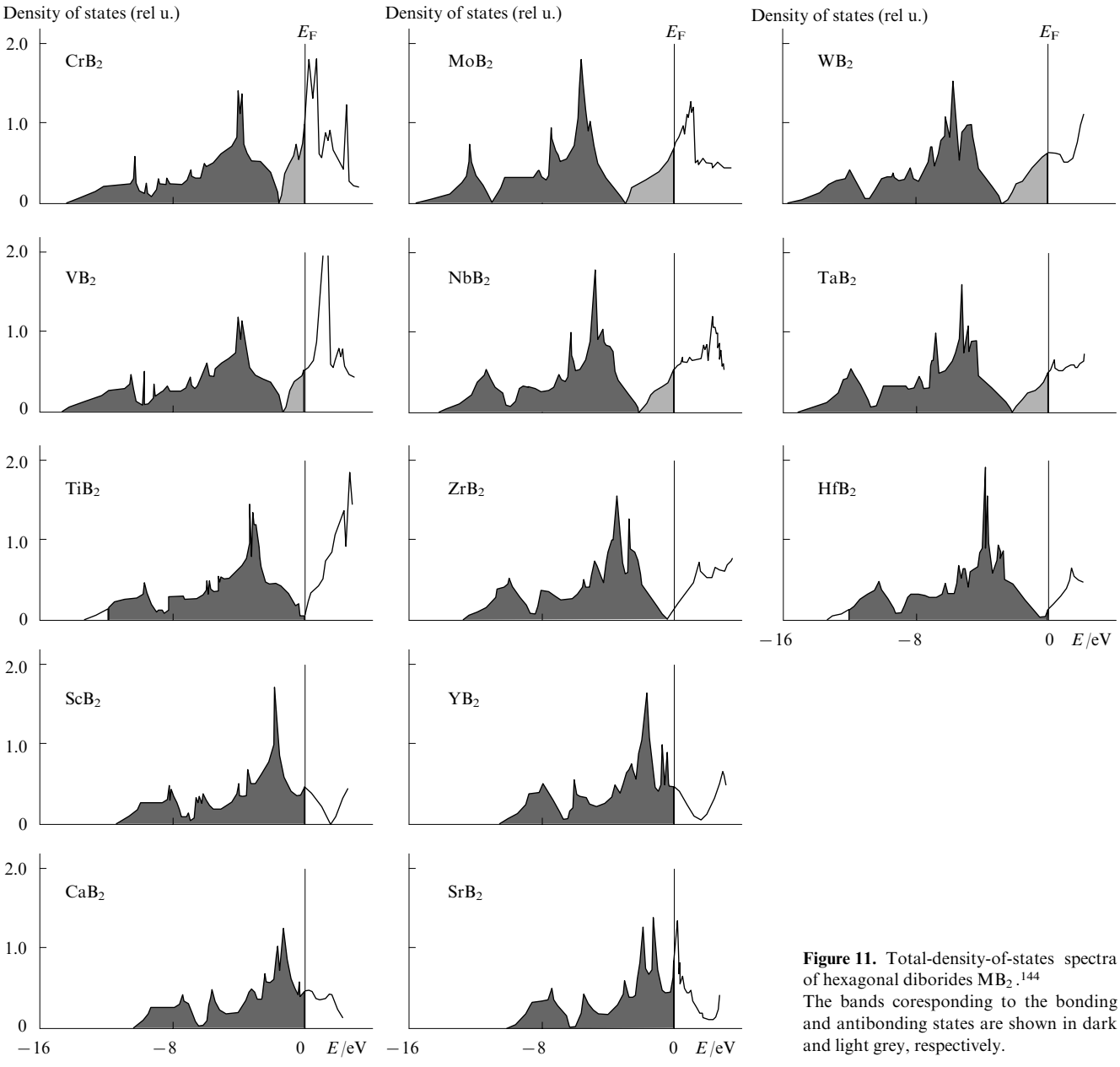


Figure 11. Total-density-of-states spectra of hexagonal diborides MB_2.[144]
The bands coresponding to the bonding and antibonding states are shown in dark and light grey, respectively.

conductivity is attributed to the low-energy shift of the σ-bands and to the absence of hole states at the Γ point (see Fig. 9). This causes changes in the topology of the Fermi surface, namely, cylinders (along the Γ – A direction) are transformed to cones. Filling of the σ-bands in AlB_2 owing to an increase in the concentration of valence electrons is responsible for the absence of superconductivity in this compound. For ScB_2 and YB_2, the p_{xy}-bands at the A point of the Brillouin zone are above E_F; however, the hole concentration is low. The Fermi levels of three diborides (TiB_2, ZrB_2 and HfB_2) are in the pseudogaps (Fig. 11). As the electron count in the Group V and VI d-metal diborides increases, the d-band is filled and $N(E_F)$ increases, which can lead to an increase in T_c. It is important that, contrary to MgB_2 transition-metal diborides are characterised by a large contribution of the metal d-states to $N(E_F)$.

Note that the stability of the diboride phases depends on the valence of the metal atom (degree of filling of valence bands), being maximum for titanium, zirconium and hafnium diborides. For these compounds, an 'optimum' condition for band filling is met, namely, all bonding states are filled while all antibonding states are vacant (see Fig. 11). An increase or decrease in the concentration of valence electrons for the Group III and V – VII metal diborides leads to filling of antibonding or depopulation of the bonding bands, respectively. This is the reason for the lower stability of these phases.

Quantum chemical calculations (Refs 12, 13, 16 – 19, 51 – 56, 59, 144, 159 – 180) revealed specific features of atom-atom interactions in diborides. It was established that the chemical bonding in these layered phases is of mixed covalent-ionic-metallic nature, being essentially anisotropic (Fig. 12). The ionic component is due to polarisation of the charge density along the M → B direction, the metallic component is due to delocalised near-Fermi electrons and the covalent component is due to the overlap of the B – B, M – M and B – M valence states within the planar boron sheets and

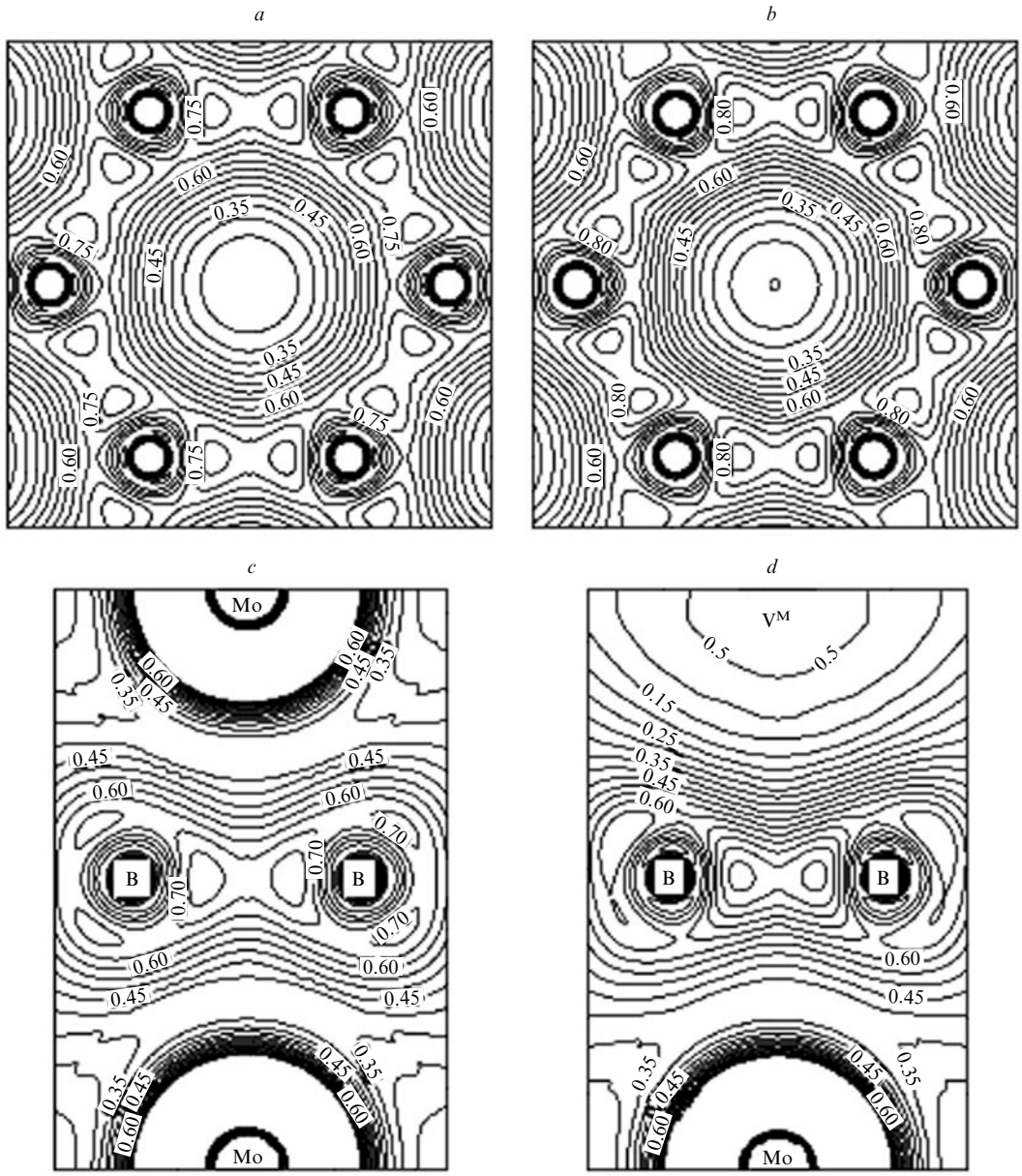


Figure 12. Valence electron density distribution in boron sheets (*a*, *b*) and in the plane normal to the boron and metal (*c*, *d*) sheets for MoB_2 (*a*, *c*) and $Mo_{0.875}B_2$ (*b*, *d*).[59] Figures at isolines denote the ρ values in $Å^{-3}$.

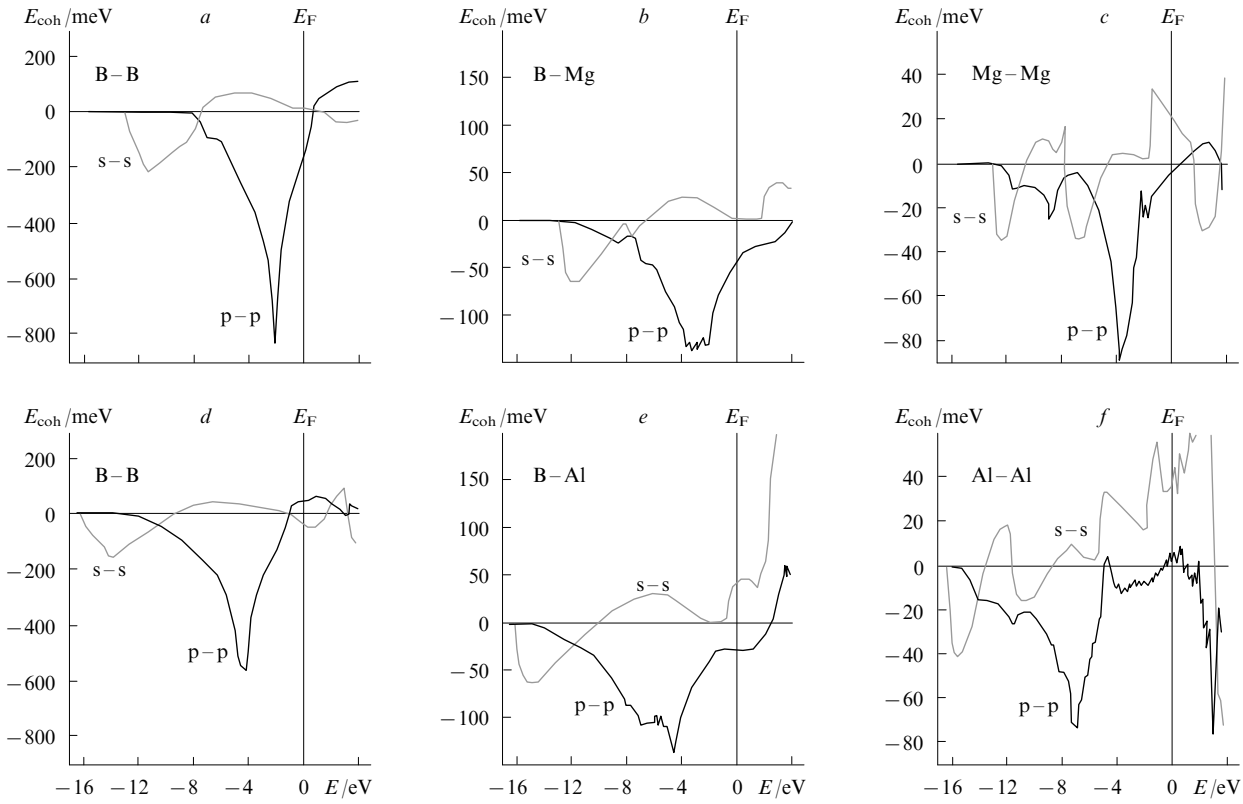


Figure 13. Partial cohesive energies of certain in-plane (*a*, *c*, *d*, *f*) and interlayer (*b*, *e*) atom-atom interactions for hexagonal MgB_2 (*a*–*c*) and AlB_2 (*d*–*f*).[169]

metal sheets between them. The strongest covalent bonds in the MB_2 crystals are formed within planar honeycomb boron sheets (Fig. 13). Estimates (Tables 2 and 3) showed that the main contribution to these bonds comes from hybridisation of the B2p–B2p orbitals.

Table 2. Energies of pair covalent bonds for MgB_2 and AlB_2 (in meV).[169]

Energy	MgB_2	AlB_2
$-E$(B–B) in-plane	2633	2453
$-E$(B–B) interlayer	18	50
$-E$(M–M) in-plane	512	567
$-E$(M–M) interlayer	37	139
$-E$(B–M)	1003	1182
$-E$(total)	4124	4325

Table 3. Contributions of particular orbitals to energies of pair covalent bonds for MgB_2 and AlB_2 (in meV).[169]

Energy	MgB_2	AlB_2
$-E$(B–B)		
p–p	1155	992
p–s	582	937
s–s	196	193
$-E$(B–M)		
p–p	339	419
p–d	180	240
p–s	174	192
s–s	49	23
$-E$(M–M)		
p–p	136	167

In addition to analysis of parameters of the electronic structure and atom–atom interactions in diborides, the results of quantum chemical calculations (Refs 12, 13, 16–19, 51–56, 59, 144, 159–180) were used to study the physicochemical properties. For instance, conditions for the onset of magnetism in MB_2 phases were studied, as well as the low-temperature electronic heat capacity coefficients (γ), lattice constants, thermodynamic and mechanical (in particular, moduli of elasticity and their derivatives) characteristics were calculated; key results are presented in Table 4.[181, 182] By and large the available results of simulation of the electronic structure and properties of defect-free MB_2 phases serve a quite reliable basis for prediction of changes in their properties in the presence of lattice vacancies.

1. Models of cation-deficient phases $M_{1-x}B_2$

Detailed information on the atomic structure (in particular, type of vacancy distribution in the metal sublattice) of the vast majority of cation-deficient phases $M_{1-x}B_2$ synthesised to date is unavailable. Theoretical simulation of such materials is carried out using two general approaches.

One of them uses the supercell model, which is well known in the energy band theory of crystals. For instance, calculations of a series of cation-deficient diborides $M_{1-x}B_2$ (M = Nb, Mo, Ag) were carried out [59, 177] using supercells $\{M_8B_{16}\}$ containing twenty-four atoms (enlargement by a factor of 8 compared to the triatomic unit cell of defect-free AlB_2-type diborides). The appearance of a cationic vacancy V^M was simulated by removing a metal atom M. Such a 'unit cell' $\{M_7V^MB_{16}\}$ corresponded to cation-deficient diborides with formal composition $M_{0.875}B_2$. It should be emphasised that the supercell model assumes an ordered vacancy distribution over the bulk of the

Table 4. Moduli of elasticity (B_0/Mbar) and their first derivatives with respect to pressure (B'_0), heats of formation (ΔH/kJ mol^{-1}), cohesive energies (E_{coh}/Rydb atom^{-1}), occupied-to-valence band width ratio (V_0/V_v), melting points (T_m/K), densities of states at the Fermi level [$N(E_F)$, Rydb^{-1}] and low-temperature susceptibility coefficients (γ/mJ mol^{-1} K^{-2}) for 3d – 5d metal diborides (results of calculations [173] and experimental data [178, 179]).

Phase	B_0 (calc.)	B_0 (exp.)	B'_0 (calc.)	$-\Delta H$ (calc.)	$-\Delta H$ (exp.)	E_{coh} (calc.)	V_0/V_v (calc.)	T_m (exp.)	$N(E_F)$ (calc.)	γ (calc.)
ScB_2	1.91	–	1.85	231.52	307	1.17	0.87	2523	11.99	2.08
TiB_2	2.13	2.02	2.1	308.38	323	1.32	1.01	3253 – 3498	4.27	0.74
VB_2	1.75	–	1.67	208.14	206	1.01	1.10	2673 – 3020	15.86	2.48
CrB_2	1.56	–	1.68	181.93	133	0.98	1.11	2473	34.88	6.05
MnB_2	2.1	–	1.65	140.04	120	0.88	1.09	2261	108.94	18.89
FeB_2	2.3	–	1.69	113.71	94.14	0.79	1.10	–	37.28	6.46
YB_2	1.41	–	2.05	101.68	105	0.88	0.86	2373	11.68	2.03
ZrB_2	1.95	2.15	1.94	296.81	322.59	1.25	1.05	3313 – 3518	3.84	0.67
NbB_2	1.01	–	1.67	192.73	197	0.94	1.17	3173 – 3309	13.95	2.42
MoB_2	1.6	–	1.71	131.61	–	0.83	1.23	2373 – 2648	20.01	3.47
HfB_2	2.16	2.1	1.35	244.20	335.98	1.21	1.05	3373 – 3653	3.688	0.64
TaB_2	1.81	–	1.78	179.15	209.20	0.98	1.12	3310 – 3473	12.92	2.24

crystal, which is specified by regular translation of the supercell.

An obvious advantage of this model is the possibility of performing a comparative analysis of various configurations of defects in the crystal. For instance, Fig. 14 presents the $Ag_6V_2^{Ag}B_{16}$ supercells in non-stoichiometric silver diboride with formal composition $Ag_{0.750}B_2$ with various types of cationic vacancy distribution. Two V^{Ag} vacancies can either occupy the neighbouring positions in the silver sublattice or be located at the maximum distance from one another (within the cell). The atomic structures comprising such supercells will be significantly different. Indeed, both inclusion of layers of metal atoms with the same number of V^{Ag} in each layer and alternation of stoichiometric and defect silver layers is possible.

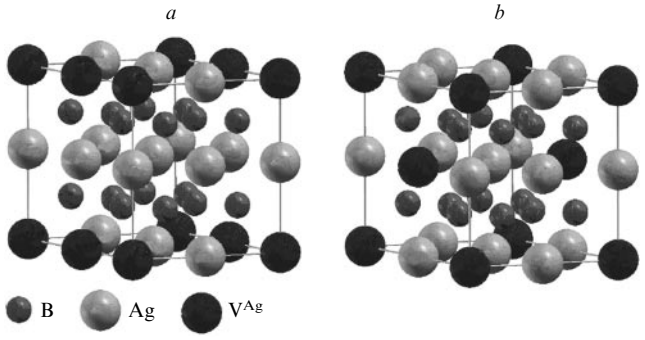


Figure 14. $Ag_6V_2^{Ag}B_{16}$ supercells simulating possible configurations of cationic vacancy distribution (V^{Ag}) in non-stoichiometric silver diboride $Ag_{0.75}B_2$.[182]
Alternation of defect and stoichiometric silver layers (*a*) and uniform distribution V^{Ag} in silver layers (*b*).

The second approach,[183] which is based on the coherent potential approximation (CPA),[184–186] is usually realised in the framework of the Green function method. Here, the Green function of a binary alloy A_cB_{1-c} is defined as follows:[187]

$$G = cG^{A,n} + (1-c)G^{B,n},$$

where $G^{A,n}$ and $G^{B,n}$ are the Green functions of the alloy components A and B, respectively. As applied to non-stoichiometric phases, this model corresponds to the case of random vacancy distribution over the corresponding sublattice in the crystal.[188–191]

A structural model of $M_{1-x}B_2$ phases [192, 193] assumes that diboride samples can be 'enriched' with boron owing to formation of vacancies in the M-sublattice and subsequent filling of this sublattice with an 'extra' boron atom, a B_2 dimer (Fig. 15) or B_3 trimer. An increase[31] in the unit cell volume of $Nb_{1-x}B_2$ with an increase in the B : Nb ratio is considered as substantiation of the model.

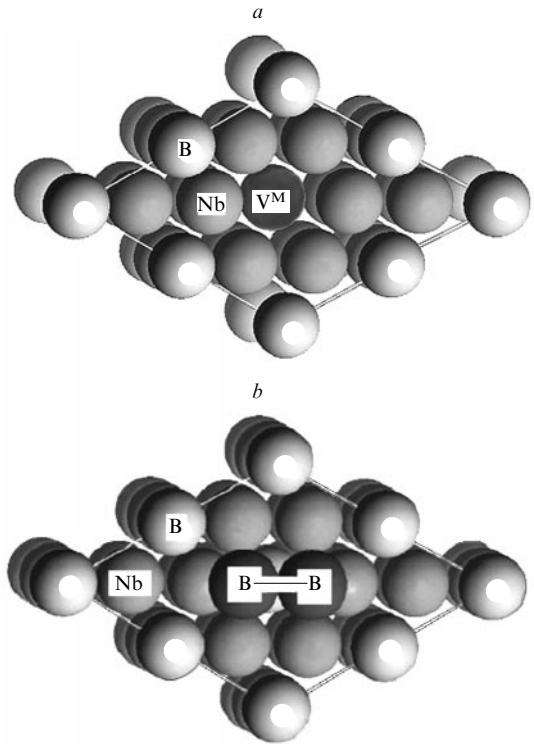


Figure 15. Models of the crystal structure of $Nb_{1-x}B_2$.[192]
Crystal with cationic vacancy (V^M) (*a*) and occupation of cationic vacancy by B_2 dimer (*b*).[192]

Below we will consider the results of calculations of the electronic structure and certain chemical properties of $M_{1-x}B_2$ phases, which were obtained using these models.

2. Electronic structure and chemical bond in cation-deficient phases $M_{1-x}B_2$

The influence of M-vacancies (V^M) on the energy band spectra of diborides $M_{0.75}B_2$ (M = Nb, Zr, Y) was carried out using the supercell model.[58] It was found that, depending on nature of the metal sublattice, the influence of M-vacancies on the energy band structure of diborides can be fundamentally different (Fig. 16). In partucular, the presence of Nb-vacancies leads to the appearance of a new peak of the density of states in the energy band spectrum of NbB_2 and to redistribution of the contributions of the Nb4d- and B2p-states near E_F. The vacancy states are below E_F on the energy scale and do not influence $N(E_F)$. Figure 17 presents the densities of states in the niobium vacancy sphere for $Nb_{0.99}B_2$. The 'vacancy states' are well known from studies of non-stoichiometric metal carbides, nitrides and oxides.[188–191, 194] Similar 'vacancy states' appear in the spectra of other d-metal diborides.

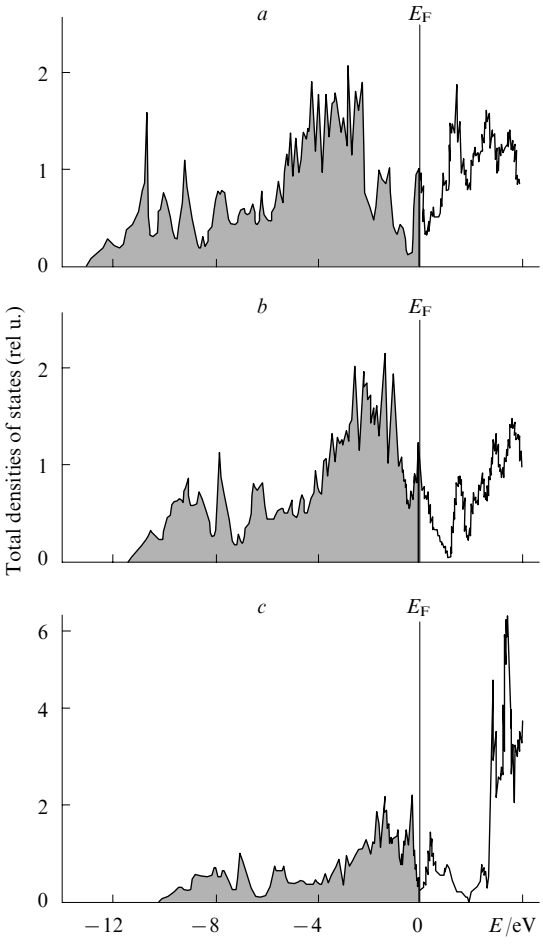


Figure 16. Total density of states spectra of cation-deficient diborides $M_{0.75}B_2$.[58]
M = Y (*a*), Zr (*b*), Nb (*c*).

Taking non-stoichiometric $Mo_{0.875}B_2$ (see Fig. 12) as an example, one can see that 'cleavage' of a number of Mo—B and Mo—Mo bonds in the formation of a Mo-vacancy leads to strengthening of B—B bonds within the boron sheet (this is the reason for the observed decrease in the parameter *a* for defect diborides, see Section II) and to partial delocalisation of the boron states in the defect region that are involved in the formation of the 'vacancy states' mentioned above.[59]

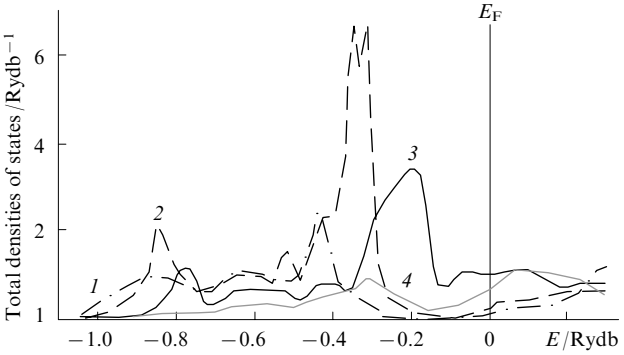


Figure 17. Density of states spectrum for the niobium vacancy sphere in $Nb_{0.99}B_2$.[183]
Shown are the s- (*1*), p- (*2*), d- (*3*) and f- (*4*) states.

Non-stoichiometry is most pronounced in the spectrum of ZrB_2; the lattice defects induce the appearance of an intense peak of the density of states in the pseudogap region.[58] $Zr_{0.75}B_2$ is characterised by an abrupt increase in both the $N(E_F)$ value and the contribution of the B2p-states (by an order of magnitude). The influence of the M-vacancies on the energy band structure of YB_2 is fundamentally different, namely, the bonding states are 'depopulated' in the presence of such vacancies; for $Y_{0.75}B_2$ the Fermi level is in a local minimum of the density of states, $N(E_F)$ and the contributions of the Y4d- and B2p-states abruptly decrease.

Thus, introduction of cationic vacancies into the metal sublattices of diborides can lead to opposite changes in the parameters of electronic spectra of MB_2 depending on the type of the metal sublattice; namely, in the presence of V^M the $N(E_F)$ value can increase (ZrB_2), vary only slightly (NbB_2) or considerably decrease (YB_2). Changes in the electron states of diborides depending on the vacancy concentration taking $Nb_{1-x}B_2$ ($0 \leqslant x \leqslant 0.3$) as an example are illustrated in Fig. 18. As can be seen, the most significant changes in the spectrum with an increase in x are due to the total decrease in the concentration of valence electrons in the system, to the corresponding shift of the Fermi level (change in the degree of filling of the bonding and antibonding bands) and to broadening of the energy bands (this is particularly pronounced at the A point of the Brillouin zone) owing to reduction of the symmetry of the system upon introduction of point defects.

3. Estimation of formation energies of cationic vacancies in $M_{1-x}B_2$ phases

Energy characteristics of non-stoichiometric systems, namely, cohesive energies (E_{coh}), energies of formation (E_f) of these phases and vacancy formation energies (E_{vf}) are important parameters that allow the effects of formation of lattice defects in metal borides to be interpreted and predicted.

The cohesive energy characterises the energy effect of 'formation' of borides from isolated atoms. The E_{coh} values are often correlated with the energy of chemical bonding in crystals. The cohesive energies of stoichiometric (MB_2) and non-stoichiometric ($M_{1-x}B_2$) diboride phases are given by

$$E_{coh}(MB_2) = E_{tot}(MB_2) - [E_{tot}(M_{at}) + 2\,E_{tot}(B_{at})],$$

$$E_{coh}(M_{1-x}B_2) = E_{tot}(M_{1-x}B_2) - [(1-x)\,E_{tot}(M_{at}) + 2\,E_{tot}(B_{at})],$$

where $E_{tot}(MB_2)$ and $E_{tot}(M_{1-x}B_2)$ are the total energies of stoichiometric and cation-deficient diborides, respectively; and

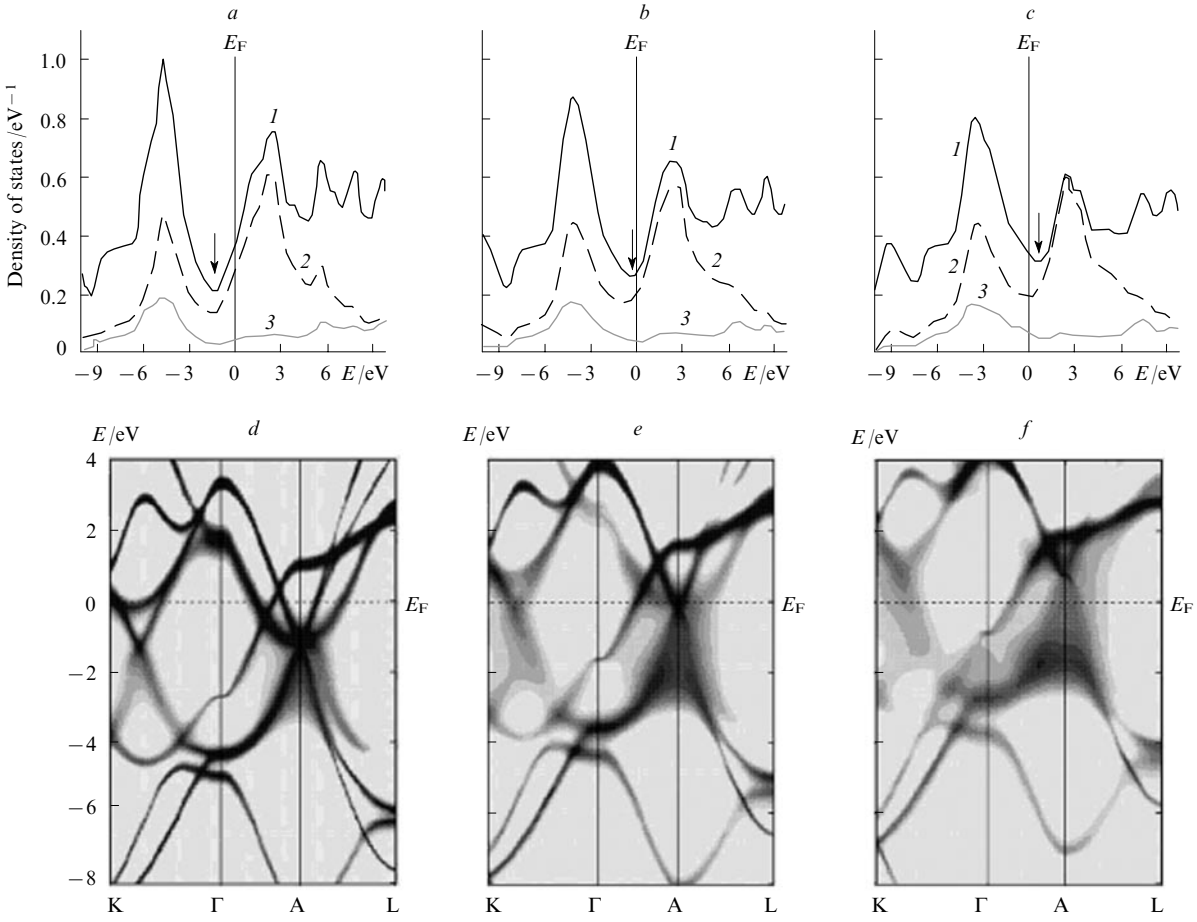


Figure 18. Densities of states (*a*–*c*) and energy band spectra (*d*–*f*) of niobium diboride at different concentration of cationic defects:[125] $Nb_{0.9}B_2$ (*a*, *d*), $Nb_{0.8}B_2$ (*b*, *e*) and $Nb_{0.7}B_2$ (*c*, *f*). Figures denote the total (*1*) and partial Nb4d- (*2*) and B2p- (*3*) densities of states.

$E_{tot}(M_{at})$ and $E_{tot}(B_{at})$ are the total energies of free (isolated) metal and boron atoms, respectively.

The formation energies (E_f) characterise the energy effect of phase formation from the starting compounds in the condensed state. Assuming that these phases are formed in the following formal reactions

$$2B + M \longrightarrow MB_2,$$

$$2B + (1-x)M \longrightarrow M_{1-x}B_2,$$

in our case the energies E_f of the stoichiometric and non-stoichiometric diboride phases can be calculated from the equations

$$E_f(MB_2) = E_{tot}(MB_2) - [E_{tot}(M_{cond}) + 2E_{tot}(B_{cond})],$$

$$E_f(M_{1-x}B_2) = E_{tot}(M_{1-x}B_2) - [(1-x)E_{tot}(M_{cond}) + 2E_{tot}(B_{cond})],$$

where $E_{tot}(M_{cond})$ and $E_{tot}(B_{cond})$ are respectively the total energies of the starting 'reactants' (crystalline metals and boron). For boron, the most stable allotrope, α-B_{12} is conventionally used.

The phase stability of compounds is governed by the Gibbs free energy

$$G = E + PV - TS.$$

Since quantum chemical calculations are usually carried out for $P = 0$ and $T = 0$, the E_f values can be interpreted as criteria for stability of the boride phases with respect to mechanical mixtures of the starting compounds in the condensed phase.

The vacancy formation energies (E_{vf}) of non-stoichiometric metal diborides can be estimated by considering the formal reaction of formation

$$MB_2 \longrightarrow M_{1-x}B_2 + xM,$$

from the equation

$$E_{vf} = E_{tot}(MB_2) - [E_{tot}(M_{1-x}B_2) + xE_{tot}(M)].$$

In this case, positive E_{vf} values indicate that the appearance of cationic vacancies in the MB_2 phases under equilibrium conditions is unfavourable. The E_{coh}, E_f and E_{vf} values calculated using modern computational quantum theory methods provide a quite reliable basis for the description of the energy of chemical bonding in crystals, for theoretical analysis of the stability of crystals, phase equilibria, *etc*. These parameters were widely used to solve these problems for many metal borides.[12, 13, 19, 49–59, 144, 145] As an example, the calculated and experimentally determined E_f values for stoichiometric hexagonal metal diborides are shown in Fig. 19. Negative E_f values correspond to stable phases, whereas for some metal compounds (mainly, formed by Group II and Group VI–VIII metals) the energies E_f take positive values, which indicates instability of the corresponding compounds. This was confirmed by experimental data on phase relations in the M–B systems.[3–11]

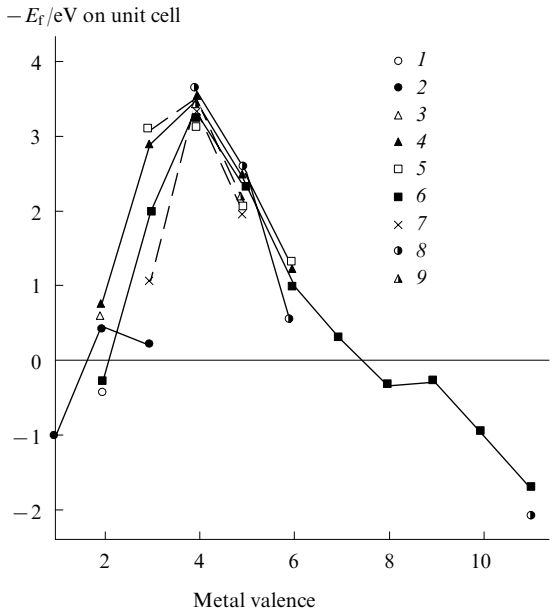


Figure 19. Calculated and experimentally determined formation energies of stoichiometric AlB_2-type metal diborides.[144]
Calculations: Be (*1*), Na – Al (*2*), Ca – Cr (*4*), Sr – Ag (*6*) and Hf – W, Au (*8*). Experimental data: Mg (*3*), Sc – Cr (*5*), Y – Nb (*7*) and Hf – Ta (*9*).

Estimates for a series of non-stoichiometric phases $M_{1-x}B_2$ are available.[58, 59, 180, 192, 193, 195] The results are shown in Tables 5 – 8.

The MB_2 phases are characterised by negative E_{coh} values. This points to stability of these systems relative to the system of noninteracting atoms (see Table 7). The maximum (in magnitude) E_{coh} values were obtained for Group IV and V d-metal diborides while the minimum cohesive energy was obtained for MgB_2. This regularity can be explained by the changes in the system of atom – atom bonds in the MB_2 phases depending on the nature of the metal atom.[195] In the general case the appearance of cationic vacancies is accompanied by cleavage of certain M – B and M – M bonds, which naturally leads to a decrease, in magnitude, of the cohesive energies of the $M_{1-x}B_2$ phases relative to the E_{coh} values of stoichiometric diborides (see Table 8).

Among stoichiometric diborides, the most stable phases are TiB_2 and ZrB_2, while AlB_2 and MgB_2 are the least stable (see Table 7). This agrees with the available data on changes in the thermodynamic and thermomechanical properties of the MB_2 phases.[3 – 11]

The following should be emphasised. For the MB_2 phases formed by the s-, p- and d-metal borides, both cohesive energy and formation energy calculations lead to the same conclusions about the phase stability ($MgB_2 < AlB_2 <$ d-metal diborides). Contrary to this, the conclusions drawn for a number of d-metal borides of similar chemical nature are opposite.[144, 195] For instance, if the energy E_{coh} decreases in magnitude in the order $NbB_2 > TaB_2 > VB_2 > ZrB_2 > TiB_2$, the formation energies of these phases change in the reverse order: $TiB_2 > ZrB_2 > VB_2 > NbB_2 > TaB_2$. This can be explained with ease[195] taking into account the fact that the minimum formation energies (for NbB_2, TaB_2) correspond to the borides based on the metals characterised by the maximum (in magnitude) cohesive energies.

Thus, the cohesive energies also characterise the stability of condensed phases. They can be used for, *e.g.*, analysis of stability of various allotropes. Correct analysis of the stability of binary crystalline phases requires calculations of the corresponding formation energies relative to the condensed forms of elements (starting reactants in the synthesis). The estimates for multicomponent phases are even more complicated and

Table 5. Calculated vacancy formation energies in metal diborides.[195]

Boride	E_{vf}/eV	Boride	E_{vf}/eV	Boride	E_{vf}/eV
$Mg_{0.75}B_2$	0.79	$Ti_{0.75}B_2$	1.57	$Zr_{0.75}B_2$	1.68
$Al_{0.75}B_2$	0.56	$V_{0.75}B_2$	0.97	$Nb_{0.75}B_2$	1.10
$Sc_{0.75}B_2$	1.46	$Y_{0.75}B_2$	1.42	$Ta_{0.75}B_2$	0.51

Table 6. Cohesive energies of stoichiometric and non-stoichiometric magnesium, zirconium and niobium diborides (in eV per formula unit).[193]

Phase [a]	$-E_{coh}$	Phase [a]	$-E_{coh}$
MgB_2	15.312	$Zr_{0.875}B_{2.125}$	22.458
$Mg_{0.875}B_2$	14.806	$Zr_{0.875}B_{2.25}$	23.594
$Mg_{0.875}B_{2.125}$	12.727	$Zr_{0.875}B_{2.375}$	24.213
$Mg_{0.875}B_{2.25}$	13.827	NbB_2	24.956
$Mg_{0.875}B_{2.375}$	14.702	$Nb_{0.875}B_2$	23.556
ZrB_2	23.628	$Nb_{0.875}B_{2.125}$	23.748
$Zr_{0.875}B_2$	22.008	$Nb_{0.875}B_{2.25}$	24.810
		$Nb_{0.875}B_{2.375}$	25.367

[a] Models of defects (compositions): vacancy in M-sublattice ($M_{0.875}B_2$); one, two and three 'super-stoichiometric' boron atoms occupying a vacancy in the M-sublattice: chemical compositions $M_{0.875}B_{2.125}$, $M_{0.875}B_{2.25}$ and $M_{0.875}B_{2.375}$, respectively.

Table 7. Cohesive energies and energies of formation of stoichiometric and cation-deficient metal diborides (in eV per formula unit).[195]

Boride	$-E_{coh}$	$-\hat{I}_f$	Boride	$-E_{coh}$	$-E_f$
MgB_2	15.10	2.21	$Mg_{0.75}B_2$	13.69	1.42
AlB_2	17.05	3.13	$Al_{0.75}B_2$	15.88	2.57
ScB_2	20.12	4.24	$S_{0.75}B_2$	17.56	2.78
TiB_2	22.98	4.89	$Ti_{0.75}B_2$	19.75	3.32
VB_2	23.67	3.84	$V_{0.75}B_2$	20.60	2.87
YB_2	19.98	3.53	$Y_{0.75}B_2$	16.70	2.11
ZrB_2	23.36	4.70	$Zr_{0.75}B_2$	19.87	3.02
NbB_2	24.84	3.73	$Nb_{0.75}B_2$	21.33	2.64
TaB_2	24.66	3.51	$Ta_{0.75}B_2$	21.73	2.99

Table 8. Lattice constants, cohesive energies, energies of formation and vacancy formation energies for stoichiometric and non-stoichiometric AlB_2-type silver diborides (in eV per formula unit).[182]

Boride [a]	a/Å	c/Å	c/a	E_{coh}	E_f	E_{vf}
AgB_2	3.024	4.085	1.3414	14.06	−0.98	–
$Ag_{0.875}B_2$	3.008	4.020	1.3364	13.71	−0.64	0.34
$Ag_{0.750}B_2$(I)	2.942	3.960	1.3460	13.32	−0.26	0.72 [b]
$Ag_{0.750}B_2$(II)	2.915	3.950	1.3551	13.33	−0.27	0.71 [b]

[a] Models I and II: $Ag_{0.750}B_2$ with different types of V^{Ag} ordering.
[b] Per two silver vacancies.

require calculations of the respective formation energies relative to those of the starting components (not only elements, but also stable binary phases that can form in these systems). For instance, a systematic analysis of the phase stability of thorium boron carbide ThB_2C should include estimates of ΔE for this phase calculated relative to (i) mechanical mixture of Th, graphite and α-B_{12} and (ii) possible binary phases formed in the Th–C–B system (ThC, ThB_6, $B_{13}C$, B_4C, BC_3 and BC_6).

The formation energy calculations for non-stoichiometric borides showed that the E_f values of $M_{0.75}B_2$ are much smaller in magnitude than those of the stoichiometric diborides (see Table 7). In other words, the presence of cationic vacancies significantly destabilises layered diborides.

Numerical estimates of the effect of destabilisation of MB_2 phases in the presence of M-vacancies can be made using calculations [195] of vacancy formation energies. According to the results listed in Table 5, diborides are characterised by positive E_{vf} values , *i.e.*, the appearance of cationic vacancies in these phases under equilibrium conditions is energetically unfavourable. The minimum E_{vf} values were obtained for the Mg, Al, Ta, Nb and V borides. As mentioned above, cation-deficient phases were synthesised for Mg, Al, Ta, Nb diborides. Calculations[190] showed that metal-deficient vanadium diboride phases can also be prepared. The formation energies of cationic vacancies for Ti, Zr, Y and Sc diborides are high, *i.e.*, the synthesis of these diborides with defects in the metal sublattice is a highly complicated task.

Energy estimates were used [182] for analysis of possible types of vacancy ordering in $Ag_{1-x}B_2$ using the models shown in Fig. 14. Analysis of the data listed in Table 8 revealed the following. First, the energy of vacancy formation in metastable silver diboride (E_{vf} = 0.34 eV) is much lower than the corresponding energies determined for other stable MB_2 phases ($E_{vf} \approx 0.51-1.68$ eV, see Table 5) in which such defects were detected experimentally. Therefore, the presence of cationic vacancies in silver diboride seems to be quite probable. Second, the vacancy distribution over all silver layers is about 0.01 eV more energetically favourable than 'clustering' of vacancies in every second layer.

Calculations of energy parameters were also used [192, 193] to analyse the possibility of filling of cationic vacancies by 'super-stoichiometric' boron (see the model in Fig. 15). It was found (see Table 6) that for non-stoichiometric magnesium diboride the maximum, in magnitude cohesive energies (*i.e.*, the most stable state of the system) correspond to the model of the crystal with cationic vacancies, whereas in the case of zirconium and niobium diborides the occupation of these vacancies by boron dimers (B_2) and trimers (B_3) favours a decrease in E_{coh} (relative to E_{coh} for a crystal with unoccupied M-sites), thus being energetically favourable.

4. Physicochemical properties of cation-deficient phases $M_{1-x}B_2$

The results of energy band structure calculations of $M_{1-x}B_2$ phases were used to determine their structural properties (equilibrium lattice constants and type of vacancy distribution),[58, 59, 125, 180, 183, 192, 193, 195] estimates of superconducting transition temperatures,[125, 183] certain parameters of electrophysical properties (*e.g.*, low-temperature heat capacity coefficients) [59] and some mechanical characteristics.

The 'elastic' parameters (bulk compression modulus, shear modulus, the Young modulus, *etc.*) belong to the most important characteristics of the mechanical properties of condensed phases and allow the behaviour of these phases under the action of various external factors to be assessed. This is of great importance for determining prospects for their use as functional materials.

Modern methods of computer materials science permit calculations of the elastic parameters of inorganic phases for not only single-crystalline, but also polycrystalline state. This makes it possible to analyse their changes depending on the phase composition and to predict the mechanical properties of polycrystalline ceramics (most metal diborides in question were prepared in this form).

Theoretical estimation of elastic parameters of non-stoichiometric metal diborides in the polycrystalline state was first reported taking NbB_{2+y} as an example.[196] NbB_{2+y} phases with $0 \leqslant y \leqslant 0.34$ were analysed; changes in the B : Nb ratio were simulated taking into account the changes in the experimentally determined lattice constant values.[36]

The first stage included calculations of the elastic constants C_{ij}. AlB_2-Type hexagonal crystals are characterised [197] by five independent constants C_{11}, C_{12}, C_{13}, C_{33}, C_{44} and C_{66}, for which one has

$$C_{66} = \frac{C_{11} - C_{12}}{2}.$$

Using these constants, the moduli of elasticity, namely, the bulk compression modulus (B) and the shear modulus (G), were determined for single-crystalline NbB_{2+y} phases according to the Voigt (V) (Ref. 198) and the Reuss (R) (Ref. 199) basic schemes:

$$B_R = \frac{C_{33}(C_{11} + C_{12}) - 2C_{13}^2}{C_{11} + C_{12} + C_{33} - 4C_{13}},$$

$$B_V = \frac{1}{9}\left[2(C_{11} + C_{12}) + C_{33} + 4C_{13}\right],$$

$$G_R = \frac{5}{2}\,\frac{[(C_{11} + C_{12})C_{33} - 2C_{13}^2]C_{55}C_{66}}{3B_RC_{55}C_{66} + [(C_{11} + C_{12})C_{33} - 2C_{12}^2]},$$

$$G_V = \frac{1}{30}(C_{11} + C_{12} + 2C_{33} - 4C_{13} + 12C_{44} + 12C_{66}).$$

Estimation of elastic parameters of polycrystalline NbB_{2+y} phases existing as aggregated mixtures of randomly oriented polycrystals requires averaging of the numerical values obtained from the calculations according to Voigt and Reuss. This was done using the Voigt–Reuss–Hill approximation (VRH) [200, 201] and the averaged bulk compression modulus

$$B_{VRH} = \frac{1}{2}(B_V + B_R),$$

shear modulus

$$G_{VRH} = \frac{1}{2}(G_V + G_R),$$

and the Young modulus (Y_{VRH}) and the Poisson ratio (v)

$$Y_{VRH} = \frac{9B_{VRH}G_{VRH}}{3B_{VRH} + G_{VRH}},$$

$$v = \frac{3B_{VRH} - 2G_{VRH}}{2(3B_{VRH} + G_{VRH})}.$$

Table 9. Independent elastic constants (C_{ij}), the Young moduli, the Poisson ratios and anisotropy coefficients for non-stoichiometric niobium borides NbB_{2+y} ($0 \leqslant y \leqslant 0.34$).[196]

B : Nb	C_{11}	C_{12}	C_{13}	C_{33}	C_{44}	Y/GPa	v	A_B (%)	A_G (%)
2.00	590	110	190	474	225	512	0.21	0.06	1.69
2.10	584	108	185	465	221	506	0.21	0.08	1.67
2.20	580	107	181	455	218	500	0.21	0.12	1.68
2.30	574	103	178	427	212	487	0.21	0.25	2.13
2.32	574	102	178	423	211	486	0.21	0.28	2.23
2.34	574	102	178	423	211	486	0.21	0.28	2.23

Elastic anisotropy of polycrystalline ceramics was also estimated. The corresponding coefficients were calculated (in %)[202]

$$A_B = \frac{B_V - B_R}{B_V + B_R},$$

$$A_G = \frac{G_V - G_R}{G_V + G_R}.$$

The coefficients can change from 0 (for isotropic systems) to 100%.

The results of calculations[191] are listed in Table 9 and shown in Fig. 20. The large and small values ($C_{13} : C_{12}$ and $C_{33} : C_{11}$, respectively) indicate a strong anisotropy of chemical bonding in niobium diboride, namely, the in-plane atom–atom interactions (bonds along the a axis) are much stronger than the interlayer interactions (bonds along the c axis). This conclusion[196] agrees with other results of analysis of chemical bonds in layered metal diborides (see above).

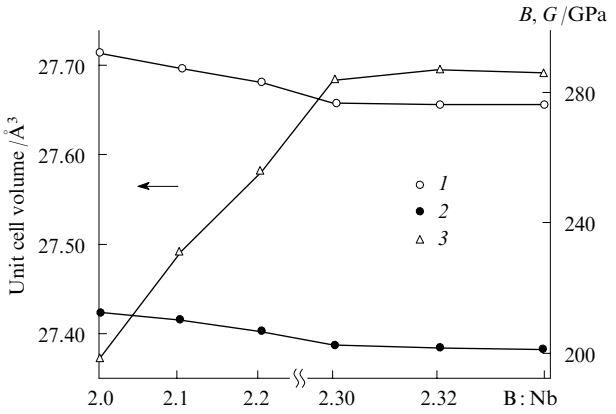


Figure 20. Bulk compression modulus (*1*), shear modulus (*2*) and the unit cell volume (*3*) plotted *vs.* B : Nb ratio in non-stoichiometric niobium borides NbB_{2+y}.[196]
Calculated using the Voigt – Reuss – Hill approximation.

The bulk compression and shear moduli of non-stoichiometric polycrystalline NbB_{2+y} samples ($0 \leqslant y \leqslant 0.34$) monotonically decrease as the B : Nb ratio increases (see Fig. 19). The $B : G$ ratio for NbB_{2+y} polycrystals is 1.37 – 1.38. At $B : G < 1.75$, the materials are brittle.[203] Therefore, niobium diboride belongs to brittle materials. The elastic anisotropy parameters (A_B and A_G) of ceramics considerably increase as the B : Nb ratio increases (see Table 9).

Note that the calculated elastic parameters are suitable for evaluation of other important properties of borides, such as the Debye temperature(θ_D)

$$\theta_D = \frac{h}{k}\left[\frac{3n}{4\pi}\left(\frac{N_A\rho}{M}\right)\right]^{1/3} \upsilon_m,$$

where n is the number of atoms in the 'molecule' of the compound, M is the molecular mass, N_A is the Avogadro constant, ρ is the density, and υ_m is the average sound velocity in the crystal, which is determined using the longitudinal (υ_l) and transverse (υ_t) sound velocities

$$\upsilon_m = \left[\frac{1}{3}\left(\frac{2}{\upsilon_t^3} + \frac{1}{\upsilon_l^3}\right)\right]^{-1/3}.$$

In turn, the υ_l and υ_t values are related to the elasticity moduli[204]

$$\upsilon_l = \sqrt{\frac{3B + 4G}{3\rho}},$$

$$\upsilon_t = \sqrt{\frac{G}{\rho}}.$$

In addition, using the calculated θ_D values and experimentally determined critical superconducting transition temperatures, one can estimate the electron–phonon coupling constant λ using McMillan's relation[205]

$$T_c = \frac{\theta_D}{1.45}\exp\left[-\frac{1.04(1+\lambda)}{\lambda - \mu^*(1+0.72\lambda)}\right],$$

where μ^* is the Coulomb pseudopotential (~ 0.13). Calculations for NbB_{2+y} showed that the λ value is about $\sim 0.50 - 0.57$.[196] This is in reasonable agreement with the estimates obtained from other calculations [~ 0.43 (Ref. 183), ~ 0.67 (Ref. 206)], which allows niobium diboride to be treated as a BKS superconductor with weak electron–phonon coupling. However, we believe that simulation[197] of changes in the chemical composition of non-stoichiometric NbB_{2+y} by changing the lattice constants alone makes it possible to consider the results only as preliminary qualitative estimates.

5. Vacancies in the boron sublattice

In conclusion, mention may be made of yet another type of lattice defects, which can be present in the phases that are formed in the metal–boron systems. These are vacancies in the boron sublattice. As mentioned above, this type of point defects is atypical of stable hexagonal MB_2 phases

At the same time, the presence of boron vacancies in metastable molybdenum diboride and molybdenum pentaboride was reported.[49] The rhombohedral phase (Mo_2B_5) includes three types of molybdenum atomic layers (*A*, *B* and *C*; see Fig. 21), which are arranged along the c axis in the order ... *AABBCCAABBCC* .... These layers are separated by two types of boron sheets, *H* and *K*. The *H*-type sheets are planar (graphite-like), while the *K*-type sheets are 'buckled' and contain more closely packed boron atoms [an extra B(3)-type boron atom is located at the centre of each B_6 hexagon].

It was reported[49] that the B(3)-type atoms can be removed from Mo_2B_5 to give the Mo_2B_{5-x} phases with non-stoichiometry in the boron sublattice. Having all B(3)-type boron atoms

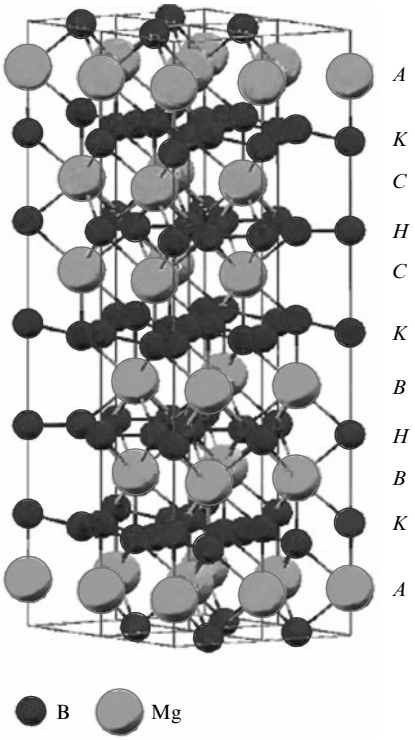


Figure 21. Structure of rhombohedral molybdenum pentaboride (Mo_2B_5).

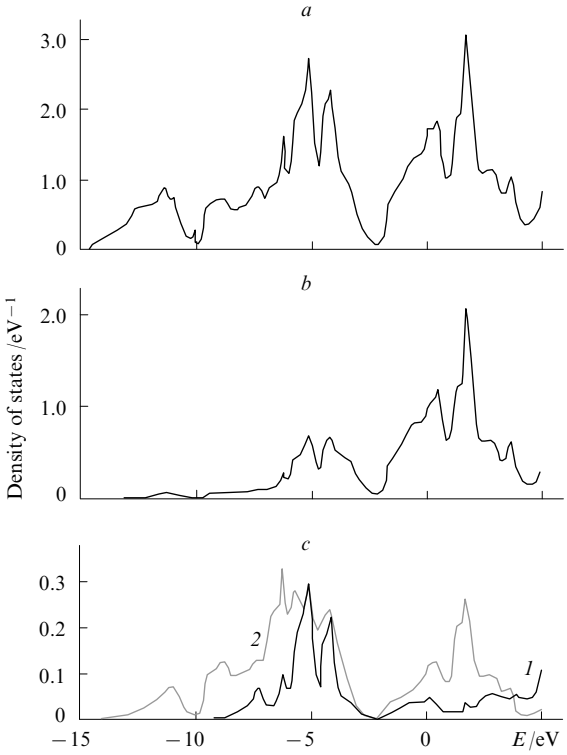


Figure 22. Total (*a*) and partial densities of Mo5d- (*b*) and B2p-states (*c*) in Mo_2B_5 with defective boron sublattice [B(3) atoms are removed, see text] of formal chemical composition $Mo_2B_4 \equiv MoB_2^r$ (Ref. 59). $B2p_x$ (*1*) and $B2p_{x+y}$ (*2*).

removed, the rhombohedral phase has the composition $Mo_2B_4 \equiv MoB_2^r$.

The electronic structure of this phase was analysed [59] (its spectrum is shown in Fig. 22). Formation energy calculations for B(3)-type vacancies using the expression

$$E_{vf} = E_{tot}(Mo_2B_5) - [E_{tot}(Mo_2B_4) + E_{tot}(B)]$$

showed that removal of these atoms from the 'buckled' boron sheets is energetically favourable ($E_{vf} = -0.11$ eV per formula unit) and the 'boron-deficient' phase $Mo_2B_4 \equiv MoB_2^r$ is more stable than Mo_2B_5 and hexagonal MoB_2.

Qualitatively, the result of stabilisation of rhombohedral Mo_2B_5 in the presence of boron vacancies can be illustrated using the distribution maps of the charge density (ρ) within the boron sheets for Mo_2B_5 and $Mo_2B_4 \equiv MoB_2^r$ (Fig. 23). As can be seen, the ρ distribution for Mo_2B_5 is delocalised in character, whereas the (ρ) distribution obtained after removal of the B(3) type atoms points to formation of strongly delocalised covalent bonds B—B. In the general case, the sixfold coordination is atypical of boron atoms (with allowance for the structure of its valence shell); while the planar structure of graphite-like boron sheets (as in hexagonal MoB_2) is energetically less favourable than the 'buckled' structure.[207] The higher stability of the newly formed $Mo_2B_4 \equiv MoB_2^r$ phase compared to Mo_2B_5 and hexagonal MoB_2 is due to formation of boron vacancies in the *K*-sheet (change in the coordination numbers of the 'remaining' boron atoms from 6 to 3) provided retention of the 'buckled' structure.[59]

Yet another group of borides includes alkaline-earth metal hexaborides MB_6 (M = Ca, Sr, Ba). Both stoichiometric (B : M = 6) and non-stoichiometric ceramics and films of these borides as well as solid solutions with isovalent substitution ($Ca_{1-x}Ba_xB_6$) exhibit weak ferromagnetism.[208–214]

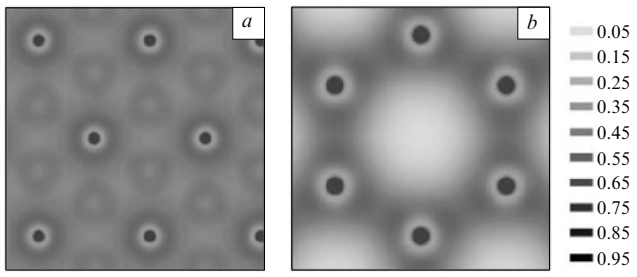


Figure 23. Charge density distribution in boron sheets for Mo_2B_5 (*K* sheet) (*a*) and $Mo_2B_4 \equiv MoB_2^r$ (*b*).[59]

Unusual effect, that is, magnetisation of non-magnetic phases (see review [215]) was attributed [216, 217] to the presence of structural vacancies in the boron sublattice. According to calculations, removal of a neutral B_6 group from the CaB_6 lattice causes the formation of a magnetic moment of about 2.36 μ_B (per $3 \times 3 \times 3$ supercell), which is localised on six B_6 octahedra that coordinate the defect in the cubic structure of CaB_{6-x}. Ferromagnetic ordering can be a consequence of 'double exchange' (Ref. 218) between magnetic clusters that form the defect in the crystal lattice and the nearest ions, Ca^{2+} and B_6^{2-}. However, the formation of defects by removal of B_6 clusters from the lattice seems to be thermodynamically unlikely. In addition, cationic vacancies can be present in a number of alkali metal hexaborides.[219] However, detailed analysis of lattice defects in these phases goes beyond the scope of this review.

IV. Conclusion

The non-stoichiometry of metal borides is a new field of research on this class of compounds. In fact, researchers have paid attention to this effect only in the 21st century in connection with rapid progress in studies of metal diborides, which followed the discovery in 2001 of superconductivity in MgB_2 with a critical transition temperature of about 39 K. It is not surprising that in most studies carried out to date the non-stoichiometry of MB_2 phases is first of all considered as a factor affecting the superconducting characteristics of the boron-containing materials.

Nevertheless, we believe that the presence of vacancies in the boride sublattices can be of general interest in connection with the fundamental problem of research on non-stoichiometry in solid-phase metal compounds and its influence of the properties of corresponding materials.

To date, many issues that have been well studied for 'classical' non-stoichiometric phases (metal carbides, nitrides and oxides) [1, 2] remain unaddressed for borides. This first of all concerns elaboration of methods of synthesis of non-stoichiometric (and, possibly, non-superconducting) metal borides, preparation of single-crystalline non-stoichiometric borides, high-precision structural studies of possible vacancy ordering effects and setting systematic theoretical and experimental studies of the role of lattice defects in the changes in the physicochemical properties of borides.

At present, non-stoichiometry of thin films and nanosized borides remains very poorly studied. It should be noted that the reasons for the appearance of 'non-stoichiometry' in such samples can be fundamentally different from the case of crystalline MB_2 samples with structural vacancies (see above). For instance, a study of 'non-stoichiometric' nanostructured $TiB_{2.4}$ films showed [220, 221] that this product consists of TiB_2 nanorods surrounded by a boron shell. In other words, in this case the term 'non-stoichiometry' was in fact used for the B/TiB_2 composite.

We believe that research on the role of non-stoichiometry of borides as components of modern multicomponent ceramics and polyfunctional composites seems to be quite promising for the design of these materials.

References

1. A I Gusev, A A Rempel, A J Margel *Disorder and Order in Strongly Non-Stoichometric Compounds: Transition Metal Carbides, Nitrides and Oxides* (Berlin, Heidelberg, New York, London: Springer, 2001)
2. A I Gusev, A A Rempel *Nestekhiometriya, Besporyadok i Poryadok v Tverdom Tele* (Non-Stoichometry, Disorder and Order in Solids) (Ekaterinburg: Urals Branch of the Russian Academy of Sciences, 2001)
3. B Post, F W Glaser *Refractory Binary Borides* (New York: Interscience, 1963)
4. A Aronsson, T Lundström, S Rundqvist *Borides, Silicides and Phosphides* (London: Methuen, 1965)
5. B Post *Refractory Binary Borides, Metallo-Boron Compounds and Boranes* (New York: Wiley, 1964)
6. H Goldschmidt *Interstitial Alloys* (London: Butterworths, 1967)
7. G V Samsonov, I M Vinitskii *Tugoplavkie Soedineniya* (Refractory Compounds) (Moscow: Metallurgiya, 1976)
8. *Boron and Refractory Borides* (Ed. M I Matkovich) (Berlin: Springer, 1977)
9. G V Samsonov, T I Serebryakova, V A Neronov *Boridy* (Borides) (Moscow: Atomizdat, 1975)
10. Yu B Kuz'ma *Kristallokhimiya Boridov* (Crystal Chemistry of Borides) (Lviv: Vishcha Shkola, 1983)
11. T I Serebryakova, V A Neronov, P D Peshev *Vysokotemperaturnye Boridy* (High-Temperature Borides) (Moscow: Metallurgiya, 1991)
12. G P Shveikin, A L Ivanovskii *Usp. Khim.* **63** 751 (1994) [*Russ. Chem. Rev.* **63** 711 (1994)]
13. A L Ivanovskii, G P Shveikin *Kvantovaya Khimiya v Materialovedenii. Bor, Ego Splavy i Soedineniya* (Quantum Chemistry in Materials Science. Boron, Its Alloys and Compounds) (Ekaterinburg: Urals Branch of the Russian Academy of Sciences, 1998)
14. J Nagamatsu, N Nakagawa, T Muranaka, Y Zenitani, J Akimitsu *Nature (London)* **410** 63 (2001)
15. C Buzea, T Yamashita *Supercond. Sci. Technol.* **14** R115 (2001)
16. A L Ivanovskii *Usp. Khim.* **70** 811 (2001) [*Russ. Chem. Rev.* **70** 717 (2001)]
17. P C Canfield, S L Bud'ko *Phys. World* **15** 29 (2002)
18. A L Ivanovskii, N I Medvedeva, V G Zubkov, V G Bamburov *Zh. Neorg. Khim.* **47** 661 (2002) [a]
19. A L Ivanovskii *Fiz. Tv. Tela* **45** 1742 (2003) [b]
20. J Akimitsu, S Akutagawa, K Kawashima, T Muranaka *Prog. Theor. Phys. Suppl.* **159** 326 (2005)
21. J Kortus *Physica C* **456** 54 (2007)
22. S Lee *Physica C* **456** 14 (2007)
23. A Floris, A Sanna, M Lüders, G Profeta, N N Lathiotakis, M A L Marques, C Franchini, E K U Gross, A Continenza, S Massidda *Physica C* **456** 45 (2007)
24. M Eisterer *Supercond. Sci. Technol.* **20** R47 (2007)
25. H Mori, S Lee, A Yamamoto, S Tajima, S Sato *Phys. Rev. V* **65** 092507 (2002)
26. V Tsirelson, A Stash, M Kohout, H Rosner, H Mori, S Sato, S Lee, A Yamamoto, S Tajima, Yu Grin *Acta Crystallogr., Sect. B* **59** 575 (2003)
27. S M Kazakov, R Puzniak, K Rogacki, A V Mironov, N D Zhigadlo, J Jun, Ch Soltman, B Batlogg, J Karpinski *Phys. Rev. B* **71** 024533 (2005)
28. R K Singh, Y Shen, R Gandikota, J M Rowell, N Newman *Supercond. Sci. Technol.* **21** 015018 (2008)
29. U Burkhardt, V Gurin, F Haarmann, H Borrmann, W Schnelle, A Yaresko, Y Grin *J. Solid State Chem.* **177** 389 (2004)
30. I Loa, K Kunc, K Syassen, P Bouvier *Phys. Rev. B* **66** 134101 (2002)
31. A Yamamoto, C Takao, T Masui, M Izumi, S Tajima *Physica C* **383** 197 (2002)
32. A S Cooper, E Corenzwit, L D Longinotti, B T Matthias, W H Zachariasen *Proc. Natl. Acad. Sci. USA* **67** 313 (1970)
33. L Leyarovska, E Layarovski *J. Less-Common Met.* **67** 249 (1979)
34. V A Gasparov, N S Sidorov, I I Zver'kov, M P Kulakov *Pis'ma Zh. Eksp. Teor. Fiz.* **73** 532 (2001) [c]
35. H Kotegawa, K Ishida, Y Kitaoka, T Muranaka, N Nakagawa, H Takagiwa, J Akimitsu *Physica C* **378–381** 25 (2002)
36. R Escamilla, O Lovera, T Akachi, A Duran, R Falconi, F Morales, R Escudero *J. Phys.: Condens. Matter* **16** 5979 (2004)
37. H Takeya, K Togano, Y S Sung, T Mochiku, K Hirata *Physica C* **408–410** 144 (2004)
38. C A Nunes, D Kaczorowski, P Rogl, M R Baldissera, P A Suzuki, G C Coelho, A Grytsiv, G Andre, F Bouree, S Okada *Acta Mater.* **53** 3679 (2005)
39. T Jarlborg *Physica B* **307** 291 (2001)
40. R Kiessling *Acta Chem. Scand.* **1** 893 (1947)
41. E F Bertaut, P Blum *Acta Crystallogr.* **4** 72 (1951)
42. I Higashi, Y Takahashi, T Atoda *J. Cryst. Growth* **33** 207 (1976)
43. I Higashi, Y Takahashi, S Okada *J. Less-Common Met.* **123** 277 (1986)
44. W Wong-Ng, H McMurdie, B Paretzkin *Powder Diffr.* **2** 112 (1987)
45. S Okada, T Atoda, I Higashi, Y Takahashi *J. Mater. Sci.* **22** 2993 (1987)
46. H Klesnar, T L Aselage, B Morosin, G H Kwei, A C Lawson *J. Alloys Compd.* **241** 180 (1996)
47. E Storms, B Mueller *J. Phys. Chem.* **81** 318 (1997)

48. K Kudaka, K Iizumi, T Sasaki, S Okada *J. Alloys Compd.* **315** 104 (2001)
49. A L Ivanovskii, N I Medvedeva, J E Medvedeva *Mendeleev Commun.* 129 (1998)
50. A L Ivanovskii, N I Medvedeva, G P Shveikin, Yu E Medvedeva, A E Nikiforov *Metallofiz. Noveishie Tekhnol.* **20** 41 (1998)
51. A L Ivanovskii, N I Medvedeva, Yu E Medvedeva *Metallofiz. Noveishie Tekhnol.* **21** 19 (1999)
52. N I Medvedeva, Yu E Medvedeva, A L Ivanovskii, V G Zubkov, A Frimen *Pis'ma Zh. Eksp. Teor. Fiz.* **71** 378 (2001) [c]
53. I R Shein, N I Medvedeva, A L Ivanovskii *Fiz. Tv. Tela* **43** 2121 (2001) [b]
54. A L Ivanovskii, N I Medvedeva *Zh. Neorg. Khim.* **45** 1234 (2000) [a]
55. N I Medvedeva, J E Medvedeva, A L Ivanovskii, A J Freeman, D L Novikov *Phys. Rev. V* **64** 020502 (2001)
56. N I Medvedeva, A L Ivanovskii, J E Medvedeva, A J Freeman, D L Novikov *Phys. Rev. B* **65** 052501 (2002)
57. I R Shein, A L Ivanovskii *Fiz. Tv. Tela* **44** 1752 (2002) [b]
58. I R Shein, N I Medvedeva, A L Ivanovskii *Fiz. Tv. Tela* **45** 1541 (2003) [b]
59. I R Shein, A L Ivanovskii *Phys. Rev. B* **73** 144108 (2006)
60. R A Andrievskii *Usp. Khim.* **66** 57 (1997) [*Russ. Chem. Rev.* **66** 53 (1997)]
61. R A Andrievski *J. Solid State Chem.* **133** 249 (1997)
62. R A Andrievskii *Usp. Khim.* **74** 1163 (2005) [*Russ. Chem. Rev.* **74** 1061 (2005)]
63. V Z Turkevich, O G Kulik, P P Itsenko, A N Sokolov, A N Lutsenko, A N Vaschenko *J. Superhard Mater.* **25** 9 (2003)
64. S Brutti, G Balducci, G Gigli, A Ciccioli, P Manfrinetti, A Palenzona *J. Cryst. Growth* **289** 578 (2006)
65. P C Canfield, D K Finnemore, S L Bud'ko, J E Ostenson, G Lapertot, C E Cunningham, C Petrovic *Phys. Rev. Lett.* **86** 2423 (2001)
66. T A Prikhna *Low Temp. Phys.* **32** 505 (2006)
67. W F Wu, Y Feng, J S Li, H P Tang, G Yan *Rare Met. Mater. Eng.* **35** 1673 (2006)
68. T Wu, J K F Yau, Y M Cai, Y G Cui, D W Gu, P F Yuan, G Q Yuan, L J Shen, X Jin *Physica C* **386** 638 (2003)
69. T S Wang, D L Yu, Z H Chi, H H Qi, Q K Hu, X G Luo, Y J Tian *J. Cryst. Growth* **299** 82 (2007)
70. Y C Liu, Q Z Shi, Q Zhao, Z Q Ma *J. Mater. Sci.: Mater. Electron.* **18** 855 (2007)
71. T Elliott, P McIntyre, A Sattarov *IEEE Trans. Appl. Supercond.* **17** 2922 (2007)
72. W Du, H Xu, H Zhang, G Zhang, D Xu, X Wang, X Hou, Y Wu, F Jiang, L Qin *J. Cryst. Growth* **289** 626 (2006)
73. W Du, D Xu, H Zhang, X Wang, G Zhang, X Hou, H Liu, Y Wang *J. Cryst. Growth* **268** 123 (2004)
74. R S Gonnelli, D,Daghero, G A Ummarino, A Calzolari, V Dellarocca, V A Stepanov, S M Jazakov, J Jun, J Karpinski *J. Phys. Chem. Solids* **67** 360 (2006)
75. E Ohmichi *Physica C* **456** 117 (2007)
76. C Krutzler, M Zehetmayer, M Eisterer, H W Weber, N D Zhigadlo, J Karpinski *Physica C* **460** 555 (2007)
77. H Bando, Y Yamaguchi, N Shirakawa, T Yanagisawa *Physica C* **412** 258 (2004)
78. J Karpinski, N D Zhigadlo, S Katrych, R Puzniak, K Rogacki, R Gonnelli *Physica C* **456** 3 (2007)
79. S R Shinde, S B Ogale, R L Greene, T Venkatesan, P C Canfield, S L Bud'ko, G Lapertot, C Petrovic *Appl. Phys. Lett.* **79** 227 (2001)
80. X X Xi, X H Zeng, A Soukiassian, J Jones, J Hotchkiss, Y Zhong, C O Brubaker, Z-K Liu, J Lettieri, D G Schlom, Y F Hu, E Wertz, Q Li, W Tian, H P Sun, X Q Pan *Supercond. Sci. Technol.* **15** 451 (2002)
81. W N Kang, H J Kim, E M Choi, C U Jung, S I Lee *Science* **292** 1521 (2001)
82. C B Eom, M R Lee, J H Choi, L J Belenky, X Song, L D Cooley, M T Naus, S Patnaik, J Jiang, M Rikel, A Polyanskii, A Gurevich, X Y Cai, S D Bu, S E Babcock, E E Hellstrom, D C Larbalestier, N Rogado, K A Regan, M A Hayward, T He, J S Slusky, K Inumaru, M K Haas, R J Cava *Nature (London)* **411** 558 (2001)
83. S H Moon, J H Yun, H N Lee, J I Kye, H G Kim, W Chung, B Oh *Appl. Phys. Lett.* **79** 2429 (2001)
84. H M Christen, H Y Zhai, C Cantoni, M Paranthaman, B C Sales, C Rouleau, D P Norton, D K Christen, D H Lowndes *Physica C* **353** 157 (2001)
85. G Grassano, W Ramadan, V Ferrando, E Bellingeri, D Marré, C Ferdeghini, G Grasso, M Putti, P Manfrinetti, A Palenzona, A Chincarini *Supercond. Sci. Technol.* **14** 762 (2001)
86. J Kim, R K Singh, N Newman, J M Rowell *IEEE Trans. Appl. Supercond.* **13** 3238 (2003)
87. Y Harada, M Uduka, Y Nakanishi, N Yoshimoto, M Yoshizawa *Physica C* **412** 1383 (2004)
88. R Schneider, J Geerk, F Ratzel, G Linker, A G Zaitsev *Appl. Phys. Lett.* **85** 5290 (2004)
89. J Albrecht, A T Matveev, J Strempfer, H-U Habermeier, D V Shantsev, Y M Galperin, T H Johansen *Phys. Rev. Lett.* **98** 117001 (2007)
90. A T Matveev, J Albrecht, M Konuma, G Cristiani, Y Krockenberger, U Starke, G Schmtz, H U Habermeier *Supercond. Sci. Technol.* **19** 299 (2006)
91. R S Hyam, K M Subhedar, S H Pawar *Appl. Surf. Sci.* **253** 1540 (2006)
92. L Crociani, G Rossetto, S Kaciulis, A Mezzi, N El-Habra, V Palmieri *Chem. Vapor Depos.* **13** 414 (2007)
93. N Peng, C Jeynes, R M Gwilliam, K J Kirkby, R P Webb *Physica C* **460** 600 (2007)
94. R A Varin, C Chiu, S Li, A Calka, D Wexler *J. Alloys Compd.* **370** 230 (2004)
95. K Kalaydjiev, V Lovchinov, D Dmitrov, M Kirov, M Baychev, C Popov, D D Radev, M Marinov, V Tumbalev, I Radev, P Vanderbemden *J. Optoelect. Adv. Mater.* **7** 423 (2005)
96. R A Varin, C Chiu *J. Alloys Compd.* **407** 268 (2006)
97. Y Zhu, L Wu, V Volkov, Q Lo, G Gu, A R Moodenbaugh, M Malac, M Suenaga, J Tranquada *Physica C* **356** 239 (2001)
98. A M Gabovich, M S Li, M Pekala, H Szymczak, A I Voitenko *Physica C* **405** 187 (2004)
99. X Y Song, V Braccini, D C Larbalestier *J. Mater. Res.* **19** 2245 (2004)
100. M Zehetmayer, M Eisterer, J Jun, S M Kazakov, J Karpinski, H W Weber *Phys. Rev. B* **70** 214516 (2004)
101. R J Cava, H W Zandbergen, K Inumaru *Physica C* **385** 8 (2003)
102. V A Drozd, A M Gabovich, P Gieriowski, M Pekala, H Szymczak *Physica C* **402** 325 (2004)
103. D G Hinks, J D Jorgensen, H Zheng, S Short *Physica C* **382** 166 (2002)
104. Y G Zhao, X P Zhang, P T Qiao, H T Zhang, S L Jia, B S Cao, M H Zhu, Z H Han, X L Wang, B L Gu *Physica C* **366** 1 (2001)
105. O Perner, J Eckert, W Hissler, C Fischer, J Acker, T Gemming, G Fuchs, B Holzapfel, L Schultz *J. Appl. Phys.* **97** 056105 (2005)
106. P A Sharma, N Hur, Y Horibe, C H Chen, B G Kim, S Guha, M Z Cieplak, S-W Cheong *Phys. Rev. Lett.* **89** 167003 (2003)
107. W A C Passos, P A Sharma, N Hur, S Guha, S-W Cheong, W A Ortiz *Physica C* **408–410** 853 (2004)
108. A E Kar'kin, V I Voronin, T V D'yachkova, N I Kadyrova, A P Tyutyunnik, V G Zubkov, Yu G Zainulin, M V Sadovskii, B N Goshchitskii *Pis'ma Zh. Eksp. Teor. Fiz.* **73** 640 (2001) [c]
109. Y Wang, F Bouquet, I Sheikin, P Toulemonde, B Revaz, M Eiaterer, H W Weber, J Hinderer, A Junrod *J. Phys.: Condens. Matter* **15** 883 (2003)
110. V Putti, V Braccini, C Ferdeghini, I Pallecchi, A F Siri, F Gatti, P Manfrinetti, A Palenzona *Phys. Rev. B* **70** 052509 (2004)
111. V Putti, V Braccini, C Ferdeghini, F Gatti, P Manfrinetti, D Marre, A Palensona, I Pallecchi, C Tarantini, I Sheikin, H U Aebersold, E B Lehmann *Appl. Phys. Lett.* **86** 112503 (2005)
112. J D Moore, G K Perkins, A D Chaplin, J Jun, S M Kazakov, J Karpinski, L F Cohen *Phys. Rev. B* **71** 224509 (2004)
113. E Mezzetti, D Botta, R Cherubini, A Chiodoni, R Gerbaldo, G Ghigo, G Giunchi, R Gozzelino, B Minetti *Physica C* **372–376** 1277 (2002)

114. N Chikumoto, A Yamamoto, M Konczykowskii, M Murakami *Physica C* **378** – **381** 466 (2002)
115. S Okayasu, H Ikeda, R Yoshizaki *Physica C* **378** – **381** 462 (2002)
116. M M A Sekkina, K M Elsabawy *Physica C* **377** 411 (2002)
117. A A Blinkin, V V Derevyanko, A N Dovbnya, T V Sukhareva, V A Finkel', I N Shlyakhov *Fiz. Tv. Tela* **48** 1921 (2006) [b]
118. X P Zhang, Y G Zhao, P T Qiao, Z S Yin, S L Jia, B S Cao, M H Zhu, Z H Han, Y H Xiong, P J Li, B L Gu *J. Supercond.* **15** 159 (2002)
119. N Rogado, M A Hayward, K A Regan, Y Y Wang, N P Ong, H W Zandbergen, J M Rowell, R Cava *J. Appl. Phys.* **91** 274 (2001)
120. R A Ribeiro, S L Bud'ko, C Petrovic, P C Canfield *Physica C* **385** 16 (2003)
121. Y Y Xue, R L Meng, B Lorenz, J K Meen, Y Y Sun, C W Chu *Physica C* **377** 7 (2002)
122. V I Matkovich, J Economy, R F Griese Jr *J. Am. Chem. Soc.* **84** 2337 (1964)
123. J Nakamura, M Watanabe, T Oguchi, S Nasubida, E Kabasawa, N Yamada, K Kuroki, H Yamazaki, S Shin, Y Umeda, S Minakawa, N Kimura, H Aoki *J. Phys. Soc. Jpn.* **71** 408 (2002)
124. A M Prokhorov, N P Lyakishev, G S Burkhanov, V A Dement'ev *Neorg. Mater.* **32** 1195 (1996) [d]
125. R J Xiao, K Q Li, H X Yang, G C Che, H R Zhang, C Ma, Z X Zhao, J Q Li *Phys. Rev. B* **73** 224516 (2006)
126. H Takagiwa, S Kuroiwa, M Yamazawa, J Akimitsu, K Ohishi, A Koda, W Higemoto, R Kadono *J. Phys. Soc. Jpn.* **74** 1386 (2005)
127. T Takasaki, T Ekino, H Takagiwa, T Muranaka, H Fujii, J Akimitsu *Physica C* **412** 266 (2004)
128. H Takeya, A Matsumoto, K Hirata, Y S Sung, K Togano *Physica C* **412** 111 (2004)
129. T Takahashi, S Kawamata, S Noguchi, T Ishida *Physica C* **426** 478 (2005)
130. R Escamilla, L Huerta *Supercond. Sci. Technol.* **19** 623 (2006)
131. C L Yeh, W H Chen *J. Alloys Compd.* **420** 111 (2006)
132. C L Yeh, W H Chen *J. Alloys Compd.* **422** 78 (2006)
133. S Kuroiwa, Y Tomita, A Sugimoto, T Ekino, J Akimitsu *J. Phys. Soc. Jpn.* **76** 094705 (2007)
134. H Nowotny, F Benesovsky, E Rudy, A Wittmann *Monatsh. Chem.* **91** 975 (1960)
135. S Okada, K Hamano, T Lundstrom, C Higashi, in *AIP Conference Proceedings on Boron-Rich Solids* Vol. 231 (Ed. D Emin) (New York: AIP, 1991) p. 456
136. E Rudy, S Windisch *Techical Reptort No. AFML-TR-65-2, Part I* Vol. X (Air Force Base, OH: Wright-Patterson, 1966)
137. B Aronsson, T Lundstrom, I Engstrom, in *Proceedings of an International Symposium on Boron-Rich Solids, Dayton, OH, 1968* p. 3
138. R Kiessling *J. Electrochem. Soc.* **98** 166 (1951)
139. L Brewer, D L Sawyer, D H Templeton, C H Dauben *J. Am. Ceram. Soc.* **34** 173 (1951)
140. H J Juretschke, R Steinitz *J. Phys. Chem. Solids* **4** 118 (1958)
141. H Itoh, Y Satoh, S Kodama, S Naka *J. Jpn. Ceram. Soc.* **98** 264 (1990)
142. X B Wang, D Tian, L Wang *J. Phys.: Condens. Matter* **6** 10185 (1994)
143. P Vajeeston, P Ravindran, C Ravi, R Asokamani *Phys. Rev. B* **63** 045115 (2001)
144. T Oguchi *J. Phys. Soc. Jpn.* **71** 1495 (2002)
145. X Hao, Z Wu, Y Xu, D Zhou, X Liu, J Meng *J. Phys.: Condens. Matter* **19** 196212 (2007)
146. L E Muzzy, M Avdeev, G Lawes, M K Haas, H W Zandbergen, A P Ramirez, J D Jorgensen, R J Cava *Physica C* **382** 153 (2002)
147. *Binary Alloy Phase Diagrams* (Ed. T B Massalski) (Materials Park, OH: ASM Int., 1990)
148. I R Shein, K I Shein, A L Ivanovskii *Physica B* **387** 184 (2007)
149. S A Kuznetsov, S V Kuznetsova, E V Rebrov, M J M Mies, M H J M de Croon, J C Schouten *Surf. Coat. Technol.* **195** 182 (2005)
150. F Yang, R S Han, N H Tong, W Guo *Chin. Phys. Lett.* **19** 1336 (2002)
151. S K Kwon, B I Min, S J Youn, K S Kim *J. Korean Phys. Soc.* **46** L1295 (2005)
152. A K M A Islam, F Parvin, F N Islam, M N Islam, A T M N Islam, I Tanaka *Physica C* **466** 76 (2007)
153. W Obrowski *Naturwissenschaften* **48** 428 (1961)
154. V N Gurin, M M Korsukova, in *Boron and Refractory Borides* (Ed. V I Matkovich) (Berlin, Heidelberg, New York: Springer, 1977) p. 301
155. M Sinder, J Pelleg cond-mat/arXiv: 0212632 (2002)
156. R Lal, V P S Awana, K P Singh, H Kishan, A V Narlikar cond-mat/arXiv: 0509674 (2005)
157. R Tomita, H Koga, T Uchiyama, I Iguchi *J. Phys. Soc. Jpn.* **73** 2639 (2004)
158. J Pelleg, M Rotman, M Sinder *Physica C* **466** 61 (2007)
159. J Kortus, I I Mazin, K D Belashchenko, V P Antropov, L L Boyer *Phys. Rev. Lett.* **86** 4656 (2001)
160. J M An, W E Pickett *Phys. Rev. Lett.* **86** 4366 (2001)
161. K D Belashchenko, M van Schilfgaarde, V P Antropov *Phys. Rev. B* **64** 092503 (2001)
162. A Y Liu, I I Mazin, J Kortus *Phys. Rev. Lett.* **87** 087005 (2001)
163. M Lmders, M A L Marques, N N Lathiotakis, A Floris, G Profeta, L Fast, A Continenza, S Massidda, E K U Gross *Phys. Rev. B* **72** 024545 (2005)
164. M A L Marques, M Lmders, N N Lathiotakis, G Profeta, A Floris, L Fast, A Continenza, E K U Gross, S Massidda *Phys. Rev. B* **72** 024546 (2005)
165. A Floris, G Profeta, N N Lathiotakis, M Lmders, M A L Marques, C Franchini, E K U Gross, A Continenza, S Massidda *Phys. Rev. Lett.* **94** 037004 (2005)
166. A K M A Islam, F N Islam, M S Iqbal, A F Jalbout, L Adamowicz *Solid State Commun.* **139** 315 (2006)
167. K Szalowski *Phys. Rev. B* **74** 094501 (2006)
168. X-R Chen, H-Y Wang, Y Cheng, Y-J Hao *Physica B* **370** 281 (2005)
169. G Bester, M Fahnle *Phys. Rev. B* **72** 094102 (2005)
170. S Souma, T Sato, T Takahashi, N Kimura, H Aoki *J. Electron Spectrosc. Relat. Phenom.* **144** 545 (2005)
171. C Paduani *Phys. Status Solidi., B* **240** 574 (2003)
172. P P Singh *Phys. Rev. Lett.* **87** 087004 (2001)
173. P Vajeeston, P Ravindran, C Ravi, R Asokamani *Phys. Rev. B* **63** 045115 (2001)
174. A K M A Islam, A S Sikder, F N Islam *Phys. Lett. A* **350** 288 (2006)
175. P de la Mora, M Castro, G Tavizon *J. Solid State Chem.* **169** 168 (2002)
176. P P Singh *Phys. Rev. B* **69** 094519 (2004)
177. H Rosner, W E Pickett, S-L Drechsler, A Handstein, G Behr, G Fuchs, K Nenkov, K-H Müller, H Eschrig *Phys. Rev. B* **64** 144516 (2001)
178. L Topor, O J Kleppa *J. Chem. Thermodyn.* **17** 1003 (1985)
179. J Samuel, Jr Schneider, in *ASM Engineering Materials Hand Book* Vol. 4 (Materials Park, OH: ASM Int., 1991) p. 790
180. H Kawanowa, R Souda, S Otani, Y Gogoh *Phys. Rev. Lett.* **81** 2264 (1998)
181. A Pallas, K Larsson *J. Phys. Chem. B* **110** 5367 (2006)
182. I R Shein N I Medvedeva, A L Ivanovskii cond-mat/arXiv: 0412426v1 (2004)
183. P J T Joseph, P P Singh *Physica C* **391** 125 (2003)
184. P Soven *Phys. Rev.* **156** 809 (1967)
185. J Faulkner *Prog. Mater. Sci.* **27** 1 (1982)
186. P P Singh, A Gonis *Phys. Rev. B* **49** 1642 (1994)
187. B L Gyorffy *Phys. Rev. B* **5** 2382 (1972)
188. E Beauprez, C F Hague, J-M Mariot, F Teyssandier, J Redinger, P Marksteiner, P Weinberger *Phys. Rev. B* **34** 886 (1986)
189. P Marksteiner, P Weinberger, A Neckel, R Zeller, P H Dederichs *Phys. Rev. B* **33** 6709 (1986)
190. J Redinger, P Marksteiner, P Weinberger *Z. Phys. B* **63** 321 (1986)

191. V I Anisimov, V P Antropov, V A Gubanov, A L Ivanovskii, E Z Kurmaev, A I Likhtenshtein, A V Postnikov *Elektronnaya Struktura Primesei i Defektov v Perekhodnykh Metallakh, ikh Splavakh i Soedineniyakh* (Electronic Structure of Impurities and Defects in Transition Metals, Their Alloys and Compounds) (Moscow: Nauka, 1989)
192. H H Farrell, R A LaViolette, T M Lillo *Physica C* **449** 1 (2006)
193. I R Shein N I Medvedeva, A L Ivanovskii cond-mat/arXiv: 0804 0894v1 (2008)
194. V A Gubanov, A L Ivanovskii, V P Zhukov *Electronic Structure of Refractory Carbides and Nitrides* (2nd Ed.) (Cambridge: Cambridge University Press, 2005)
195. I R Shein, A L Ivanovskii *Zh. Neorg. Khim.* **52** 95 (2007) [a]
196. E Regalado, R Escamilla *J. Phys.: Condens. Matter* **19** 376209 (2007)
197. J F Nye *Physical Properties of Crystal* (Oxford: Clarendon Press, 1985)
198. W Voigt *Lehrbuch der Kristallphysik* (Leipzig: Teubner, 1928)
199. A Reuss *Z. Angew. Math. Mech.* **9** 49 (1929)
200. R Hill *Proc. Phys. Soc.* **65** 349 (1952)
201. Q Chen, B Sundman *Acta Mater.* **49** 947 (2001)
202. D H Chung, W R Buessem, F W Vahldiek *Anisotropy in Single Crystal Refractory Compounds* (Ed. S A Mersol) (New York: Plenum, 1968)
203. S F Pugh *Philos. Mag.* **45** 833 (1954)
204. E Schreiber, O L Anderson, N Soga *Elastic Constants and Their Measurements* (New York: McGraw-Hill, 1973)
205. W L McMillan *Phys. Rev.* **167** 331 (1968)
206. R Heid, B Renker, H Schober, P Adelmann, D Ernst, K-P Bohnen *Phys. Rev. B* **67** 180510 (2003)
207. M H Evans, J D Joannopoulos, S T Pantelides *Phys. Rev. B* **72** 045434 (2005)
208. D P Young, D Hall, M E Torelli, Z Fisk, J D Thomson, H R Ott, S B Oseroff, R G Goodrich, R Zysler *Nature (London)* **397** 412 (1999)
209. H R Ott, J L Gavilano, B Ambrosini, P Vonlanthen, E Felder, L Degiorgi, D P Young, Z Fisk, R Zysler *Physica B* **281**–**282** 423 (2000)
210. P Vonlanthen, E Felder, L Degiorgi, H R Ott, D P Young, A D Bianchi, Z Fisk *Phys. Rev. B* **62** 10076 (2000)
211. M C Bennett, J van Lierop, E M Berkeley, J F Mansfield, C Henderson, M C Aronson, D P Young, A Bianchi, Z Fisk, F Balakirev, A Lacerda *Phys. Rev. B* **69** 132407 (2004)
212. T Moriwaka, T Nishioka, N K Sato *J. Phys. Soc. Jpn.* **70** 341 (2001)
213. J S Rhyee, B K Cho *J. Appl. Phys.* **95** 6675 (2004)
214. M H Cao, Y K Sun, J Jiang, H X Liu, J Yuan *J. Inorg. Mater.* **21** 640 (2006)
215. A L Ivanovskii *Usp. Fiz. Nauk* **177** 1083 (2007) [*Physics-Uspekhi* **50** 1031 (2007)]
216. T Jarlborg *J. Phys.: Condens. Matter* **15** L249 (2003)
217. R Monnier, B Delley *Phys. Rev. Lett.* **87** 157204 (2001)
218. P W Anderson, H Hasegawa *Phys. Rev.* **100** 675 (1955)
219. S V Okatov, A L Ivanovskii *Phys. Status Solidi B* **222** R6 (2000)
220. P H Mayrhofer, C Mitterer, H Clemens *Adv. Eng. Mater.* **7** 1071 (2005)
221. P H Mayrhofer, C Mitterer, J G Wen, J E Greene, I Petrov *Appl. Phys. Lett.* **86** 131909 (2005)

[a] — *Russ. J. Inorg. Chem. (Engl. Transl.)*
[b] — *Phys. Solid State (Engl. Transl.)*
[c] — *J. Exp. Theor. Phys. Lett. (Engl. Transl.)*
[d] — *Inorg. Mater. (Engl. Transl.)*